3 Magnetism in Correlated Matter

Eva Pavarini
Institute for Advanced Simulation
Forschungszentrum Jülich

Contents

E. Pavarini, E. Koch, and P. Coleman (eds.)
Many-Body Physics: From Kondo to Hubbard
Modeling and Simulation Vol. 5
Forschungszentrum Jülich, 2015, ISBN 978-3-95806-074-6
http://www.cond-mat.de/events/correl15

1 Overview

Around the beginning of last century magnetic phenomena in materials were at the center of a hot scientific debate: What causes ferromagnetic order? At the time, atoms were not fully understood, and there were perhaps more questions than answers. Weiss proposed the molecular mean-field theory of ferromagnetism [1], which dominated the scene. Friedrich Hund formulated his now-famous rules [2] to determine the atomic ground-state multiplets, which turned out to be basically exact. Heisenberg [3] realized that Coulomb exchange leads to ferromagnetic coupling between local magnetic moments. New puzzles emerged. Can other types of long-range order occur in Nature? In 1949 the first observation of antiferromagnetic order was reported, causing a great sensation [4]. Such a state had been predicted by Néel [5] about 20 years before via an extended version of Weiss' mean-field theory. In the mean-time, however, it was clear that the theory had a problem. Indeed, antiferromagnetism was an artifact of the static mean-field approximation. Bethe [6] had found the general solution of the one-dimensional Heisenberg spin chain, which shows that, in the case of antiferromagnetic coupling between the spins, the ground state has a total spin zero, and thus it is not the antiferromagnetic state. Several years later, Anderson understood [7] that the original $SU(2)$ symmetry of the Hamiltonian in spin space, broken in the antiferromagnetic state, is recovered once quantum fluctuations are taken into account; this lead to broken-symmetry theory and ultimately to the postulation of the famous Anderson-Higgs boson [8, 9]. While all this was happening, other effects that involved local magnetic moments were discovered. A low-temperature minimum in the resistance of some metals puzzled scientists for long, until in 1964 Kondo understood [10] that it is caused by local spins (magnetic impurities) coupled antiferromagnetically to conduction-electron spins. The theoretical efforts to understand the Kondo effect, described via the Kondo model or the more general Anderson model, fueled the development of new powerful non-perturbative many-body techniques, among which the numerical renormalization group. Experimentally, many f-electron compounds were identified as lattices of Kondo impurities. In 1975, the discovery of a huge electronic specific heat in $CeAl_3$ below 0.2 K [11] brought a new category of strongly correlated materials to light, the heavy fermions [12]. These are dense Kondo systems with low-temperature Fermi liquid properties but extremely large quasielectron masses. To complicate the scenario, in such materials the Kondo effect competes with long-range magnetic order, and both phenomena are mediated by the same interaction. Furthermore, several members of the heavy-fermion family, such as $CeCu_2Si_2$, become unconventional superconductors at low temperature. Later on in 1986, a novel class of unconventional superconductors, high-temperature superconducting cuprates, was found [13]; these systems are believed to be doped Mott insulators, described, at least to first approximation, by the two-dimensional single-band Hubbard model. Around the same time, with the development of the dynamical mean-field theory (DMFT) [14], it emerged that the Anderson model and the Kondo effect are intimately connected with the Mott metal-insulator transition [15, 16] and thus with the Hubbard model. In these lecture notes we will discuss some of the models and methods that made this exciting piece of the history of modern physics [12, 15–22].

Magnetism ultimately arises from the intrinsic magnetic moment of electrons, $\boldsymbol{\mu} = -g\mu_B \boldsymbol{s}$, where μ_B is the Bohr magneton and $g \simeq 2.0023$ is the electronic g-factor. It is, however, an inherently quantum mechanical effect, the consequence of the interplay between the Pauli exclusion principle, the Coulomb electron-electron interaction, and the hopping of electrons. To understand this let us consider the simplest possible system, an isolated atom or ion. In the non-relativistic limit electrons in a single ion are typically described by the Hamiltonian

$$H_e^{\mathrm{NR}} = -\frac{1}{2}\sum_i \nabla_i^2 - \sum_i \frac{Z}{r_i} + \sum_{i>j} \frac{1}{|\boldsymbol{r}_i - \boldsymbol{r}_j|},$$

where Z is the atomic number and $\{\boldsymbol{r}_i\}$ are the coordinates of the electrons with respect to the ionic nucleus. Here, as in the rest of this lecture, we use atomic units. If we consider only the external atomic shell with quantum numbers nl, for example the $3d$ shell of transition-metal ions, we can rewrite this Hamiltonian as follows

$$H_e^{\mathrm{NR}} = \varepsilon_{nl} \sum_{m\sigma} c^\dagger_{m\sigma} c_{m\sigma} + \frac{1}{2}\sum_{\sigma\sigma'} \sum_{m\tilde{m}m'\tilde{m}'} U^l_{mm'\tilde{m}\tilde{m}'} c^\dagger_{m\sigma} c^\dagger_{m'\sigma'} c_{\tilde{m}'\sigma'} c_{\tilde{m}\sigma}. \tag{1}$$

The parameter ε_{nl} is the energy of the electrons in the nl atomic shell and m the degenerate one-electron states in that shell. For a hydrogen-like atom

$$\varepsilon_{nl} = -\frac{1}{2}\frac{Z^2}{n^2}.$$

The couplings $U^l_{mm'\tilde{m}\tilde{m}'}$ are the four-index Coulomb integrals. In a basis of atomic functions the bare Coulomb integrals are

$$U^{iji'j'}_{mm'\tilde{m}\tilde{m}'} = \int d\boldsymbol{r}_1 \int d\boldsymbol{r}_2 \, \frac{\overline{\psi_{im\sigma}}(\boldsymbol{r}_1)\overline{\psi_{jm'\sigma'}}(\boldsymbol{r}_2)\psi_{j'\tilde{m}'\sigma'}(\boldsymbol{r}_2)\psi_{i'\tilde{m}\sigma}(\boldsymbol{r}_1)}{|\boldsymbol{r}_1 - \boldsymbol{r}_2|},$$

and $U^l_{mm'\tilde{m}\tilde{m}'} = U^{iiii}_{mm'\tilde{m}\tilde{m}'}$, where $m, m', \tilde{m}, \tilde{m}' \in nl$ shell. The eigenstates of Hamiltonian (1) for fixed number of electrons N are the multiplets [23,24]. Since in H_e^{NR} the Coulomb repulsion and the central potential are the only interactions, the multiplets can be labeled with S and L, the quantum numbers of the electronic total spin and total orbital angular momentum operators, $\boldsymbol{S} = \sum_i \boldsymbol{s}_i$, and $\boldsymbol{L} = \sum_i \boldsymbol{l}_i$. Closed-shell ions have $S = L = 0$ in their ground state. Ions with a partially-filled shell are called *magnetic ions*; the value of S and L for their ground state can be obtained via Hund's rules. The first and second Hund's rules say that the lowest-energy multiplet is the one with

1. the largest value of S
2. the largest value of L compatible with the previous rule

The main relativistic effect is the spin-orbit interaction, which has the form $H_e^{\mathrm{SO}} = \sum_i \lambda_i \, \boldsymbol{l}_i \cdot \boldsymbol{s}_i$. For not-too-heavy atoms it is a weak perturbation. For electrons in a given shell, we can rewrite H_e^{SO} in a simpler manner using the first and second Hund's rule. If the shell filling is $n < 1/2$,

the ground-state multiplet has spin $S = (2l+1)n = N/2$; thus $\boldsymbol{s}_i = \boldsymbol{S}/N = \boldsymbol{S}/2S$. If, instead, $n > 1/2$, since the sum of $\boldsymbol{l}_i$ vanishes for the electrons with spin parallel to $\boldsymbol{S}$, only the electrons with spin antiparallel to $\boldsymbol{S}$ contribute. Their spin is $\boldsymbol{s}_i = -\boldsymbol{S}/N_u = -\boldsymbol{S}/2S$ where $N_u = 2(2l+1)(1-n)$ is the number of unpaired electrons. We therefore obtain the LS Hamiltonian

$$H_e^{\rm SO} \sim \underbrace{\left[2\Theta(1-2n)-1\right] \frac{g\mu_B^2}{2S} \left\langle \frac{1}{r}\frac{d}{dr} v_{\rm R}(r) \right\rangle}_{\lambda} \boldsymbol{L}\cdot\boldsymbol{S} = \lambda\, \boldsymbol{L}\cdot\boldsymbol{S}, \tag{2}$$

where Θ is the Heaviside step function and $v_{\rm R}(r)$ is the effective potential, which includes, e.g., the Hartree electron-electron term [25]. For a hydrogen-like atom, $v_{\rm R}(r) = -Z/r$. Because of the LS coupling (2) the eigenstates have quantum numbers L, S and J, where $\boldsymbol{J} = \boldsymbol{S} + \boldsymbol{L}$ is the total angular momentum. Since $\boldsymbol{L}\cdot\boldsymbol{S} = \left[\boldsymbol{J}^2 - \boldsymbol{L}^2 - \boldsymbol{S}^2\right]/2$, the value of J in the ground-state multiplet is thus (third Hund's rule)

- total angular momentum $J = \begin{cases} |L-S| & \text{for filling } n < 1/2 \\ S & \text{for filling } n = 1/2 \\ L+S & \text{for filling } n > 1/2 \end{cases}$

In the presence of spin-orbit interaction a given multiplet is then labeled by ${}^{2S+1}L_J$, and its states can be indicated as $|JJ_zLS\rangle$. If we consider, e.g., the case of the Cu^{2+} ion, characterized by the [Ar] $3d^9$ electronic configuration, Hund's rules tell us that the $3d$ ground-state multiplet has quantum numbers $S = 1/2$, $L = 2$ and $J = 5/2$. A Mn^{3+} ion, which is in the [Ar] $3d^4$ electronic configuration, has instead a ground-state multiplet with quantum numbers $S = 2$, $L = 2$ and $J = 0$. The order of the Hund's rules reflects the hierarchy of the interactions. The strongest interactions are the potential $v_{\rm R}(r)$, which determines ε_{nl}, and the average Coulomb interaction, the strength of which is measured by the average *direct Coulomb integral*,

$$U_{\rm avg} = \frac{1}{(2l+1)^2} \sum_{mm'} U^l_{mm'mm'}.$$

For an N-electron state the energy associated with these two interactions is $E(N) = \varepsilon_{nl} N + U_{\rm avg} N(N-1)/2$, the same for all multiplets of a given shell. The first Hund's rule is instead due to the average *exchange Coulomb integral*, $J_{\rm avg}$, defined as

$$U_{\rm avg} - J_{\rm avg} = \frac{1}{2l(2l+1)} \sum_{mm'} \left(U^l_{mm'mm'} - U^l_{mm'm'm}\right),$$

which is the second-largest Coulomb term; for transition-metal ions $J_{\rm avg} \sim 1$ eV. Smaller Coulomb integrals determine the orbital anisotropy of the Coulomb matrix and the second Hund's rule.[1] The third Hund's rule comes, as we have seen, from the spin-orbit interaction which, for not-too-heavy atoms, is significantly weaker than all the rest.

[1] For more details on Coulomb integrals and their averages see Ref. [25].

The role of Coulomb electron-electron interaction in determining S and L can be understood through the simple example of a C atom, electronic configuration [He] $2s^2\ 2p^2$. We consider only the p shell, filled by two electrons. The Coulomb exchange integrals have the form

$$J^p_{m,m'} = U^p_{mm'm'm} = \int d\boldsymbol{r}_1 \int d\boldsymbol{r}_2 \ \frac{\overline{\psi_{im\sigma}}(\boldsymbol{r}_1)\overline{\psi_{im'\sigma}}(\boldsymbol{r}_2)\psi_{im\sigma}(\boldsymbol{r}_2)\psi_{im'\sigma}(\boldsymbol{r}_1)}{|\boldsymbol{r}_1 - \boldsymbol{r}_2|}$$
$$= \int d\boldsymbol{r}_1 \int d\boldsymbol{r}_2 \ \frac{\phi_{imm'\sigma}(\boldsymbol{r}_1)\overline{\phi_{imm'\sigma}}(\boldsymbol{r}_2)}{|\boldsymbol{r}_1 - \boldsymbol{r}_2|}. \tag{3}$$

If we express the Coulomb potential as

$$\frac{1}{|\boldsymbol{r}_1 - \boldsymbol{r}_2|} = \frac{1}{V}\sum_{\boldsymbol{k}} \frac{4\pi}{k^2} e^{i\boldsymbol{k}\cdot(\boldsymbol{r}_1 - \boldsymbol{r}_2)},$$

we can rewrite the Coulomb exchange integrals in a form that shows immediately that they are always positive

$$J^p_{m,m'} = \frac{1}{V}\sum_{\boldsymbol{k}} \frac{4\pi}{k^2} \left|\phi_{imm'\sigma}(\boldsymbol{k})\right|^2 > 0.$$

They generate the Coulomb-interaction term

$$-\frac{1}{2}\sum_{\sigma}\sum_{m\neq m'} J^p_{m,m'} c^\dagger_{m\sigma} c_{m\sigma} c^\dagger_{m'\sigma} c_{m'\sigma} = -\frac{1}{2}\sum_{m\neq m'} 2J^p_{m,m'}\left[S^m_z S^{m'}_z + \frac{1}{4} n_m n_{m'}\right].$$

This exchange interaction yields an *energy gain* if the two electrons occupy two different p orbitals with parallel spins, hence it favors the state with the largest spin (first Hund's rule). It turns out that for the p^2 configuration there is only one possible multiplet with $S = 1$, and such a state has $L = 1$. There are instead two excited $S = 0$ multiplets, one with $L = 0$ and the other with $L = 2$; the latter is the one with lower energy (second Hund's rule).
To understand the magnetic properties of an isolated ion we have to analyze how its levels are modified by an external magnetic field $\boldsymbol{h}$. The effect of a magnetic field is described by

$$H^{\mathrm{H}}_e = \mu_B\left(g\boldsymbol{S} + \boldsymbol{L}\right)\cdot\boldsymbol{h} + \frac{h^2}{8}\sum_i \left(x_i^2 + y_i^2\right) = H^{\mathrm{Z}}_e + H^L_e. \tag{4}$$

The linear term is the Zeeman Hamiltonian. If the ground-state multiplet is characterized by $J \neq 0$ the Zeeman interaction splits its $2J + 1$ degenerate levels. The second-order term yields Larmor diamagnetism, which is usually only important if the ground-state multiplet has $J = 0$, as happens for ions with closed external shells. The energy $\mu_B h$ is typically very small (for a field as large as 100 T it is as small as 6 meV); it can however be comparable with or larger than the spin-orbit interaction if the latter is tiny (very light atoms). Taking all interactions into account, the total Hamiltonian is

$$H_e \sim H^{\mathrm{NR}}_e + H^{\mathrm{SO}}_e + H^{\mathrm{H}}_e.$$

In a crystal the electronic Hamiltonian is complicated by the interaction with other nuclei and their electrons. The non-relativistic part of the Hamiltonian then takes the form

$$H_e^{\rm NR} = -\frac{1}{2}\sum_i \nabla_i^2 + \frac{1}{2}\sum_{i\neq i'} \frac{1}{|\boldsymbol{r}_i - \boldsymbol{r}_{i'}|} - \sum_{i\alpha} \frac{Z_\alpha}{|\boldsymbol{r}_i - \boldsymbol{R}_\alpha|} + \frac{1}{2}\sum_{\alpha\neq\alpha'} \frac{Z_\alpha Z_{\alpha'}}{|\boldsymbol{R}_\alpha - \boldsymbol{R}_{\alpha'}|},$$

where Z_α is the atomic number of the nucleus located at position $\boldsymbol{R}_\alpha$. In a basis of localized Wannier functions [25] this Hamiltonian can be written as

$$H_e^{\rm NR} = -\sum_{ii'\sigma}\sum_{mm'} t^{i,i'}_{m,m'} c^\dagger_{im\sigma} c_{i'm'\sigma} + \frac{1}{2}\sum_{ii'jj'}\sum_{\sigma\sigma'}\sum_{mm'}\sum_{\tilde{m}\tilde{m}'} U^{iji'j'}_{mm'\tilde{m}\tilde{m}'} c^\dagger_{im\sigma} c^\dagger_{jm'\sigma'} c_{j'\tilde{m}'\sigma'} c_{i'\tilde{m}\sigma}, \quad (5)$$

where

$$t^{i,i'}_{m,m'} = -\int d\boldsymbol{r}\, \overline{\psi_{im\sigma}}(\boldsymbol{r}) \left[-\frac{1}{2}\nabla^2 + v_{\rm R}(\boldsymbol{r})\right] \psi_{i'm'\sigma}(\boldsymbol{r}).$$

The terms $\varepsilon_{m,m'} = -t^{i,i}_{m,m'}$ yield the crystal-field matrix and $t^{i,i'}_{m,m'}$ with $i \neq i'$ the hopping integrals. The label m indicates here the orbital quantum number of the Wannier function. In general, the Hamiltonian (5) will include states stemming from more than a single atomic shell. For example, in the case of strongly correlated transition-metal oxides, the set $\{im\}$ includes transition-metal $3d$ and oxygen $2p$ states. The exact solution of the many-body problem described by (5) is an impossible challenge. The reason is that the properties of a many-body system are inherently emergent and hence hard to predict *ab-initio* in the absence of any understanding of the mechanism behind them. In this lecture, however, we want to focus on magnetism. Since the nature of cooperative magnetic phenomena in crystals is currently to a large extent understood, we can find realistic approximations to (5) and even map it onto simpler models that still retain the essential ingredients to explain long-range magnetic order.

Let us identify the parameters of the electronic Hamiltonian important for magnetism. The first is the crystal-field matrix $\varepsilon_{m,m'}$. The crystal field at a given site i is a non-spherical potential due to the joint effect of the electric field generated by the surrounding ions and of covalent-bond formation [24]. The crystal field can split the levels within a given shell and therefore has a strong impact on magnetic properties. We can identify three ideal regimes. In the *strong-crystal-field* limit the crystal-field splitting is so large that it is comparable with the average Coulomb exchange responsible for the first Hund's rule. This can happen in $4d$ or $5d$ transition-metal oxides. A consequence of an *intermediate crystal field* (weaker than the average Coulomb exchange but larger than Coulomb anisotropy and spin-orbit interaction) is the quenching of the angular momentum, $\langle \boldsymbol{L}\rangle = 0$. In this limit the second and third Hund's rule are not respected. This typically happens in $3d$ transition-metal oxides. In $4f$ systems the crystal-field splitting is usually much weaker than the spin-orbit coupling (*weak-crystal-field* limit) and mainly splits states within a given multiplet, leaving a reduced magnetic moment. In all three cases, because of the crystal field, a magnetic ion in a crystal might lose – totally or partially – its spin, its angular momentum, or its total momentum. Or, sometimes, it is the other way around. This happens for Mn^{3+} ions, which should have a $J = 0$ ground state according to the third Hund's rule. In the perovskite $LaMnO_3$, however, they behave as $S = 2$ ions because of the quenching of the angular momentum.

Even if the crystal field does not suppress the magnetic moment of the ion, the electrons might delocalize to form broad bands, completely losing their original atomic character. This happens, e.g., if the hopping integrals $t^{i,i'}_{m,m'}$ are much larger than the average on-site Coulomb interaction $U_{\rm avg}$. Surprisingly, magnetic instabilities arise even in the absence of localized moments. This *itinerant magnetism* is mostly due to band effects, i.e., it is associated with a large one-electron linear static response-function $\chi_0(\boldsymbol{q};0)$. In this limit correlation effects are typically weak. To study them we can exploit the power of the *standard model* of solid-state physics, the density-functional theory (DFT), taking into account Coulomb interaction effects beyond the local-density approximation (LDA) at the perturbative level, e.g., in the random-phase approximation (RPA). With this approach we can understand and describe Stoner instabilities.
In the opposite limit, the *local-moments* regime, the hopping integrals are small with respect to $U_{\rm avg}$. This is the regime of strong electron-electron correlations, where complex many-body effects, e.g., those leading to the Mott metal-insulator transition, play an important role. At *low enough energy*, however, only spins and spin-spin interactions matter. Ultimately, at integer filling we can integrate out (*downfold*) charge fluctuations and describe the system via effective spin Hamiltonians. The latter typically take the form

$$H_{\rm S} = \frac{1}{2}\sum_{ii'} \Gamma^{i,i'}\ \boldsymbol{S}_i \cdot \boldsymbol{S}_{i'} + \cdots = H^H_{\rm S} + \ldots . \tag{6}$$

The term $H^H_{\rm S}$ given explicitly in (6) is the Heisenberg Hamiltonian, and $\Gamma^{i,i'}$ is the Heisenberg exchange coupling, which can be antiferromagnetic ($\Gamma^{i,i'} > 0$) or ferromagnetic ($\Gamma^{i,i'} < 0$). The Hamiltonian (6) can, for a specific system, be quite complicated, and might include long-range exchange interactions or anisotropic terms. Nevertheless, it represents a huge simplification compared to the unsolvable many-body problem described by (5), since, at least within very good approximation schemes, it can be solved. Spin Hamiltonians of type (6) are the minimal models that still provide a realistic picture of long-range magnetic order in strongly correlated insulators. There are various sources of exchange couplings. Electron-electron repulsion itself yields, via Coulomb exchange, a ferromagnetic Heisenberg interaction, the *Coulomb exchange interaction*. The origin of such interaction can be understood via a simple model with a single orbital, m. The inter-site Coulomb exchange coupling has then the form

$$J^{i,i'} = U^{ii'i'i}_{mmmm} = \int d\boldsymbol{r}_1 \int d\boldsymbol{r}_2\ \frac{\overline{\psi_{im\sigma}}(\boldsymbol{r}_1)\overline{\psi_{i'm\sigma}}(\boldsymbol{r}_2)\psi_{im\sigma}(\boldsymbol{r}_2)\psi_{i'm\sigma}(\boldsymbol{r}_1)}{|\boldsymbol{r}_1 - \boldsymbol{r}_2|},$$

and it is therefore positive, as one can show by following the same steps that we used in Eq. (3) for $J^p_{m,m'}$. Hence, the corresponding Coulomb interaction yields a ferromagnetic Heisenberg-like Hamiltonian with

$$\Gamma^{i,i'} = -2J^{i,i'} < 0.$$

A different source of magnetic interactions are the *kinetic exchange* mechanisms (direct exchange, super-exchange, double exchange, Ruderman-Kittel-Kasuya-Yosida interaction ...), which are mediated by the hopping integrals. Kinetic exchange couplings are typically (with

a few well understood exceptions) antiferromagnetic [26]. A representative example of kinetic exchange will be discussed in the next section.
While the itinerant and local-moment regime are very interesting ideal limiting cases, correlated materials elude rigid classifications. The same system can present features associated with both regimes, although at different temperatures and/or energy scales. This happens in Kondo systems, heavy fermions, metallic strongly correlated materials, and doped Mott insulators.
In this lecture we will discuss in representative cases the itinerant and localized-moment regime and their crossover, as well as the most common mechanisms leading to magnetic cooperative phenomena. Since our target is to understand strongly correlated materials, we adopt the formalism typically used for these systems. A concise introduction to Matsubara Green functions, correlation functions, susceptibilities, and linear-response theory can be found in the Appendix.

2 The Hubbard model

The simplest model that we can consider is the one-band Hubbard model

$$H = \underbrace{\varepsilon_d \sum_i \sum_\sigma c^\dagger_{i\sigma} c_{i\sigma}}_{H_d} \underbrace{-t \sum_{\langle ii'\rangle} \sum_\sigma c^\dagger_{i\sigma} c_{i'\sigma}}_{H_T} + \underbrace{U \sum_i n_{i\uparrow} n_{i\downarrow}}_{H_U} = H_d + H_T + H_U, \tag{7}$$

where ε_d is the on-site energy, t is the hopping integral between first-nearest neighbors $\langle ii'\rangle$, and U the on-site Coulomb repulsion; $c^\dagger_{i\sigma}$ creates an electron in a Wannier state with spin σ centered at site i, and $n_{i\sigma} = c^\dagger_{i\sigma} c_{i\sigma}$. The Hubbard model is a simplified version of Hamiltonian (5) with $m = m' = \tilde{m} = \tilde{m}' = 1$ and

$$\begin{cases} \varepsilon_d &= -t^{i,i}_{1,1} \\ t &= t^{\langle i,i'\rangle}_{1,1} \\ U &= U^{iiii}_{1111} \end{cases}.$$

In the $U = 0$ limit the Hubbard model describes a system of independent electrons. The Hamiltonian is then diagonal in the Bloch basis

$$H_d + H_T = \sum_{\boldsymbol{k}\sigma} \Big[\varepsilon_d + \varepsilon_{\boldsymbol{k}}\Big] c^\dagger_{\boldsymbol{k}\sigma} c_{\boldsymbol{k}\sigma}. \tag{8}$$

The energy dispersion $\varepsilon_{\boldsymbol{k}}$ depends on the geometry and dimensionality d of the lattice. For a hypercubic lattice of dimension d

$$\varepsilon_{\boldsymbol{k}} = -2t \sum_{\nu=1}^{d} \cos(k_{r_\nu} a),$$

where a is the lattice constant, and $r_1 = x, r_2 = y, r_3 = z$. The energy $\varepsilon_{\boldsymbol{k}}$ does not depend on the spin. In Fig. 1 we show $\varepsilon_{\boldsymbol{k}}$ in the one-, two- and three-dimensional cases.

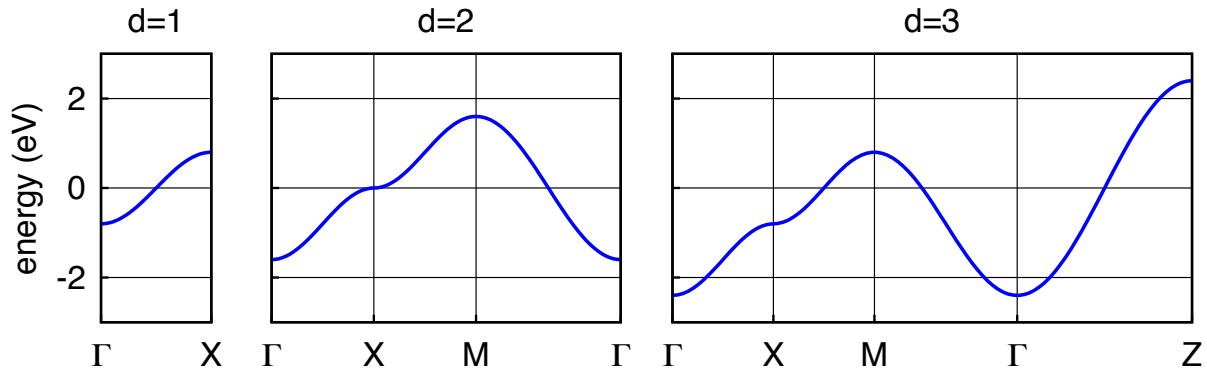

Fig. 1: *The band structure of the one-band tight-binding model (hypercubic lattice). The hopping integral is $t = 0.4$ eV. From left to right: one-, two-, and three-dimensional case. At half filling ($n = 1$) the Fermi level is at zero energy.*

In the opposite limit ($t = 0$) the Hubbard model describes a collection of isolated atoms. Each atom has four electronic many-body states

$$\begin{array}{lcl|ccc} |N,S,S_z\rangle & & & N & S & E(N) \\ \hline |0,0,0\rangle & = & |0\rangle & 0 & 0 & 0 \\ |1,\tfrac{1}{2},\uparrow\rangle & = & c^\dagger_{i\uparrow}|0\rangle & 1 & 1/2 & \varepsilon_d \\ |1,\tfrac{1}{2},\downarrow\rangle & = & c^\dagger_{i\downarrow}|0\rangle & 1 & 1/2 & \varepsilon_d \\ |2,0,0\rangle & = & c^\dagger_{i\uparrow}c^\dagger_{i\downarrow}|0\rangle & 2 & 0 & 2\varepsilon_d + U \end{array} \tag{9}$$

where $E(N)$ is the total energy, N the total number of electrons and S the total spin. We can express the atomic Hamiltonian $H_d + H_U$ in a form in which the dependence on N_i, S_i, and S^i_z is explicitly given

$$H_d + H_U = \varepsilon_d \sum_i n_i + U \sum_i \left[-\left(S^i_z\right)^2 + \frac{n_i^2}{4} \right], \tag{10}$$

where $S^i_z = (n_{i\uparrow} - n_{i\downarrow})/2$ is the z component of the spin operator and $n_i = \sum_\sigma n_{i\sigma} = N_i$.
In the large t/U limit and at half filling we can downfold charge fluctuations and map the Hubbard model into an effective spin model of the form

$$H_S = \frac{1}{2}\Gamma \sum_{\langle ii'\rangle} \left[\boldsymbol{S}_i \cdot \boldsymbol{S}_{i'} - \frac{1}{4} n_i n_{i'} \right]. \tag{11}$$

The coupling Γ can be calculated by using second-order perturbation theory. For a state in which two neighbors have opposite spin, $|\uparrow,\downarrow\rangle = c^\dagger_{i\uparrow}c^\dagger_{i'\downarrow}|0\rangle$, we obtain the energy gain

$$\Delta E_{\uparrow\downarrow} \sim -\sum_I \langle\uparrow,\downarrow|H_T|I\rangle\langle I \left| \frac{1}{E(2) + E(0) - 2E(1)} \right| I\rangle\langle I|H_T|\uparrow,\downarrow\rangle \sim -\frac{2t^2}{U}.$$

Here $|I\rangle$ ranges over the excited states with one of the two neighboring sites doubly occupied and the other empty, $|\uparrow\downarrow,0\rangle = c^\dagger_{i\uparrow}c^\dagger_{i\downarrow}|0\rangle$, or $|0,\uparrow\downarrow\rangle = c^\dagger_{i'\uparrow}c^\dagger_{i'\downarrow}|0\rangle$; these states can be occupied via virtual hopping processes. For a state in which two neighbors have parallel spins, $|\uparrow,\uparrow\rangle = c^\dagger_{i\uparrow}c^\dagger_{i'\uparrow}|0\rangle$, no virtual hopping is possible because of the Pauli principle, and $\Delta E_{\uparrow\uparrow} = 0$. Thus

$$\frac{1}{2}\Gamma \sim (\Delta E_{\uparrow\uparrow} - \Delta E_{\uparrow\downarrow}) = \frac{1}{2}\frac{4t^2}{U}. \tag{12}$$

The exchange coupling $\Gamma = 4t^2/U$ is positive, i.e., antiferromagnetic.
Canonical transformations [28] provide a scheme for deriving the effective spin model systematically at any perturbation order. Let us consider a unitary transformation of the Hamiltonian

$$H_S = e^{iS}He^{-iS} = H + [iS,H] + \frac{1}{2}\Big[iS,[iS,H]\Big] + \dots .$$

We search for a transformation operator that eliminates, at a given order, hopping integrals between states with a different number of doubly occupied states. To do this, first we split the kinetic term H_T into a component H_T^0 that does not change the number of doubly occupied states and two terms that either increase it (H_T^+) or decrease it (H_T^-) by one

$$H_T = -t\sum_{\langle ii'\rangle}\sum_\sigma c^\dagger_{i\sigma}c_{i'\sigma} = H_T^0 + H_T^+ + H_T^-,$$

where

$$H_T^0 = -t\sum_{\langle ii'\rangle}\sum_\sigma n_{i-\sigma}\; c^\dagger_{i\sigma}c_{i'\sigma}\; n_{i'-\sigma} - t\sum_{\langle ii'\rangle}\sum_\sigma \Big[1-n_{i-\sigma}\Big]c^\dagger_{i\sigma}c_{i'\sigma}\Big[1-n_{i'-\sigma}\Big],$$

$$H_T^+ = -t\sum_{\langle ii'\rangle}\sum_\sigma n_{i-\sigma}\; c^\dagger_{i\sigma}c_{i'\sigma}\Big[1-n_{i'-\sigma}\Big],$$

$$H_T^- = \left(H_T^+\right)^\dagger .$$

The term H_T^0 commutes with H_U. The remaining two terms fulfill the commutation rules

$$[H_T^\pm, H_U] = \mp U H_T^\pm .$$

The operator S can be expressed as a linear combination of powers of the three operators H_T^0, H_T^+, and H_T^-. The actual combination, which gives the effective spin model at a given order, can be found via a recursive procedure [28]. At half filling and second order, however, we can simply guess the form of S that leads to the Hamiltonian (11). By defining

$$S = -\frac{i}{U}\left(H_T^+ - H_T^-\right)$$

we obtain

$$H_S = H_U + H_T^0 + \frac{1}{U}\Big(\left[H_T^+,H_T^-\right] + \left[H_T^0,H_T^-\right] + \left[H_T^+,H_T^0\right]\Big) + \mathcal{O}(U^{-2}).$$

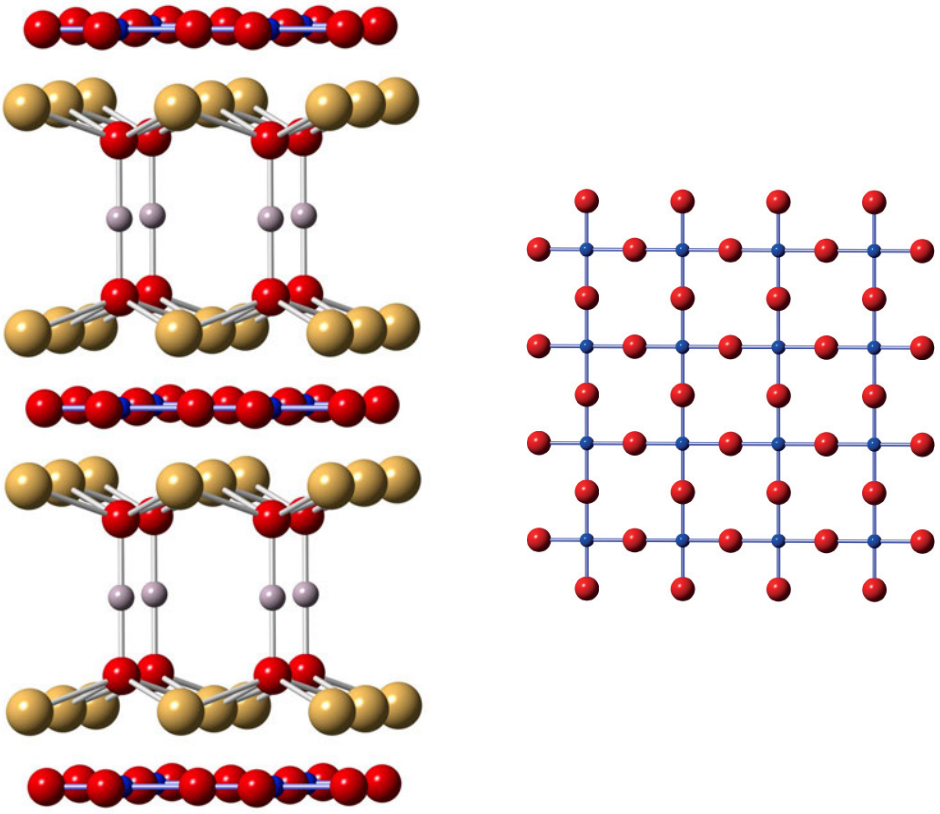

Fig. 2: *Left: The crystal structure of $HgBa_2CuO_4$ showing the two-dimensional CuO_2 layers. Spheres represent atoms of Cu (blue), O (red), Ba (yellow), and Hg (grey). Right: A CuO_2 layer. The first-nearest-neighbor hopping integral between neighboring Cu sites t is roughly given by $\sim 4t_{pd}^2/\Delta_{dp}$, where t_{pd} is the hopping between Cu d and O p states and $\Delta_{dp} = \varepsilon_d - \varepsilon_p$ their charge-transfer energy.*

If we restrict the Hilbert space of H_S to the subspace with one electron per site (half filling), no hopping is possible without increasing the number of occupied states; hence, only the term $H_T^- H_T^+$ contributes. After some algebra, we obtain $H_S = H_S^{(2)} + \mathcal{O}(U^{-2})$ with

$$H_S^{(2)} = \frac{1}{2}\frac{4t^2}{U}\sum_{ii'}\left[\boldsymbol{S}_i \cdot \boldsymbol{S}_{i'} - \frac{1}{4}n_i n_{i'}\right].$$

The Hubbard model (7) is rarely realized in Nature in this form. To understand real materials one typically has to take into account orbital degrees of freedom, long-range hopping integrals, and sometimes longer-range Coulomb interactions or perhaps even more complex many-body terms. Nevertheless, there are very interesting systems whose low-energy properties are, to first approximation, described by (7). These are strongly correlated organic crystals (one-dimensional case) and high-temperature superconducting cuprates, in short HTSCs (two-dimensional case). An example of HTSC is $HgBa_2CuO_4$, whose structure is shown in Fig. 2. It is made of CuO_2 planes well divided by BaO-Hg-BaO blocks. The $x^2 - y^2$-like states stemming from the CuO_2 planes can be described via a one-band Hubbard model. The presence of a $x^2 - y^2$-like band at the Fermi level is a common feature of all HTSCs.

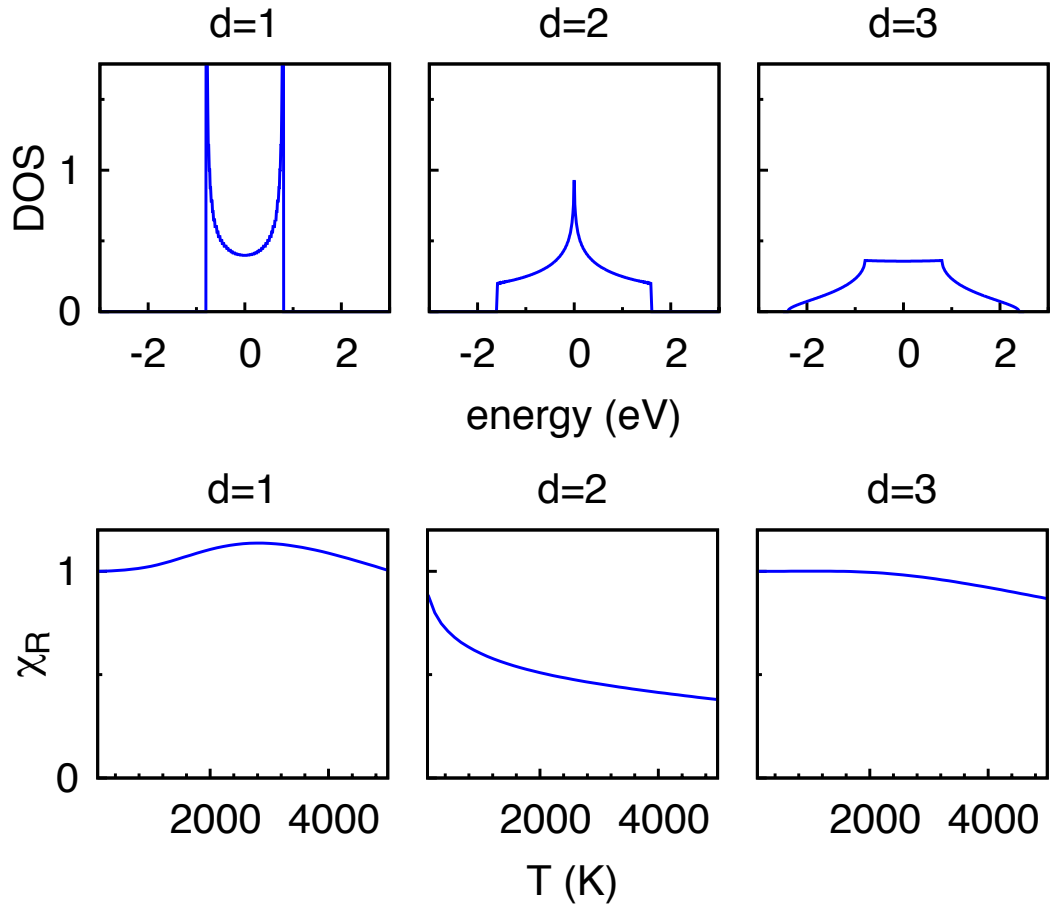

Fig. 3: *Top: Density of states (DOS) per spin, $\rho(\varepsilon)/2$, for a hypercubic lattice in one, two, and three dimensions. The energy dispersion is calculated for $t = 0.4$ eV. The curves exhibit different types of Van-Hove singularities. Bottom: Effect of $\rho(\varepsilon_F)$ on the temperature dependence of $\chi_R = \chi^P(T)/\chi^P(0)$. Up to $\sim$ 1000 K only the logarithmic Van-Hove singularity (two-dimensional case) yields a sizable effect.*

2.1 Weak-correlation limit

2.1.1 The $U = 0$ case: Pauli paramagnetism

Let us consider first the non-interacting limit of the Hubbard model, Hamiltonian (8). In the presence of an external magnetic field $\boldsymbol{h} = h_z\hat{z}$ the energy $\varepsilon_{\boldsymbol{k}}$ of a Bloch state is modified by the Zeeman interaction (4) as follows

$$\varepsilon_{\boldsymbol{k}} \to \varepsilon_{\boldsymbol{k}\sigma} = \varepsilon_{\boldsymbol{k}} + \frac{1}{2}\sigma g\mu_B h_z,$$

where we take the direction of the magnetic field as quantization axis and where on the right-hand side $\sigma = 1$ or -1 depending if the spin is parallel or antiparallel to $\boldsymbol{h}$. Thus, to linear order in the magnetic field, the $T = 0$ magnetization of the system is

$$M_z = -\frac{1}{2}(g\mu_B)\frac{1}{N_{\boldsymbol{k}}}\sum_{\boldsymbol{k}}\left[n_{\boldsymbol{k}\uparrow} - n_{\boldsymbol{k}\downarrow}\right] \sim \frac{1}{4}\left(g\mu_B\right)^2\rho(\varepsilon_F)h_z,$$

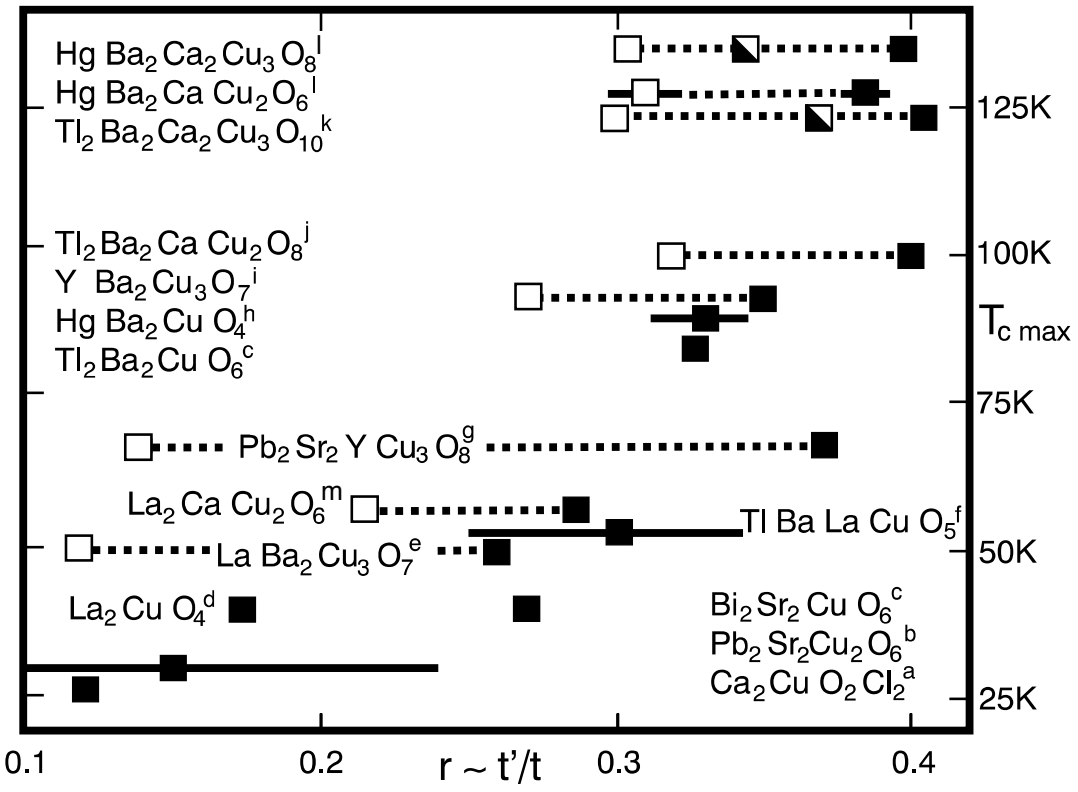

Fig. 4: *Band-structure trend in hole-doped cuprates and correlation with $T_{c\,\max}$, the maximum value of the critical temperature for superconductivity. From Ref. [29].*

where $n_{\boldsymbol{k}\sigma} = \langle c^\dagger_{\boldsymbol{k}\sigma} c_{\boldsymbol{k}\sigma} \rangle$ and $N_{\boldsymbol{k}}$ is the number of $\boldsymbol{k}$ points; $\rho(\varepsilon_F)$ is the total density of states (DOS) at the Fermi level ε_F. The $T = 0$ susceptibility is then given by the Pauli formula

$$\chi^P(0) = \frac{1}{4} (g\mu_B)^2 \rho(\varepsilon_F).$$

In linear-response theory (see Appendix) the magnetization induced along $\hat{z}$ by an external magnetic field $h_z(\boldsymbol{q};\omega)\hat{z}$ oscillating with vector $\boldsymbol{q}$ is given by

$$M_z(\boldsymbol{q};\omega) = \chi_{zz}(\boldsymbol{q};\omega) h_z(\boldsymbol{q};\omega).$$

The Pauli susceptibility $\chi^P(0)$ is thus the static ($\omega = 0$) and uniform ($\boldsymbol{q} = \boldsymbol{0}$) linear response function to an external magnetic field. At finite temperature the Pauli susceptibility takes the form

$$\chi^P(T) = \frac{1}{4} (g\mu_B)^2 \int d\varepsilon \rho(\varepsilon) \left(-\frac{dn(\varepsilon)}{d\varepsilon} \right),$$

where $n(\varepsilon) = 1/(1 + e^{(\varepsilon-\mu)\beta})$ is the Fermi distribution function, $\beta = 1/k_B T$, and μ the chemical potential. $\chi^P(T)$ depends weakly on the temperature; its temperature dependence is more pronounced, however, in the presence of Van-Hove singularities close to the Fermi level (Fig. 3).

2.1.2 The Fermi liquid regime

In *some* limit the independent-particle picture still holds even when the Coulomb interaction is finite. Landau's phenomenological Fermi liquid theory suggests that, at low-enough energy and temperature, the elementary excitations of a weakly interacting system can be described by almost independent fermionic quasiparticles, fermions with effective mass m^* and finite lifetime $\tau^{\rm QP}$

$$\varepsilon^{\rm QP}_{n\boldsymbol{k}} = \frac{m}{m^*}\varepsilon_{n\boldsymbol{k}},$$
$$\tau^{\rm QP} \propto (aT^2 + b\omega^2)^{-1}.$$

Remarkably, a very large number of materials do exhibit low-energy Fermi liquid behavior, and the actual violation of the Fermi liquid picture is typically an indication that something surprising is going on. How are quasiparticles related to actual particles, however? Landau postulated that the low-lying states of a weakly-correlated system are well-described by the energy functional

$$E = E_0 + \sum_{\boldsymbol{k}\sigma} \varepsilon_{\boldsymbol{k}\sigma}\delta n_{\boldsymbol{k}\sigma} + \frac{1}{2}\sum_{\boldsymbol{k}\sigma}\sum_{\boldsymbol{k}'\sigma'} f_{\boldsymbol{k}\sigma\boldsymbol{k}'\sigma'}\delta n_{\boldsymbol{k}\sigma}\delta n_{\boldsymbol{k}'\sigma'},$$

where E_0 is the ground-state energy, $\delta n_{\boldsymbol{k}\sigma} = n_{\boldsymbol{k}\sigma} - n^0_{\boldsymbol{k}\sigma}$ gives the number of quasiparticles (or quasi-holes), $n_{\boldsymbol{k}\sigma}$ is the occupation number in the excited state, and $n^0_{\boldsymbol{k}\sigma}$ is the occupation number of the non-interacting system at $T = 0$. The idea behind this is that $\delta n_{\boldsymbol{k}\sigma}$ is small with respect to the number of particles and therefore can be used as an expansion parameter. The low-lying elementary excitations are thus fermions with dispersion

$$\varepsilon^{\rm QP}_{n\boldsymbol{k}} = \frac{\delta E}{\delta n_{\boldsymbol{k}\sigma}} = \varepsilon_{\boldsymbol{k}\sigma} + \sum_{\boldsymbol{k}'\sigma'} f_{\boldsymbol{k}\sigma\boldsymbol{k}'\sigma'}\delta n_{\boldsymbol{k}'\sigma'},$$

so that

$$E = E_0 + \sum_{\boldsymbol{k}\sigma} \varepsilon^{\rm QP}_{n\boldsymbol{k}}\delta n_{\boldsymbol{k}\sigma},$$

i.e., the energy of quasiparticles is additive. Remarkably, by definition

$$f_{\boldsymbol{k}\sigma\boldsymbol{k}'\sigma'} = \frac{\delta^2 E}{\delta n_{\boldsymbol{k}\sigma}\delta n_{\boldsymbol{k}'\sigma'}}.$$

Hence, $f_{\boldsymbol{k}\sigma\boldsymbol{k}'\sigma'}$ is symmetric in all the arguments. If the system has inversion symmetry, $f_{\boldsymbol{k}\sigma\boldsymbol{k}'\sigma'} = f_{-\boldsymbol{k}\sigma-\boldsymbol{k}'\sigma'}$; furthermore, if the system has time-reversal symmetry, $f_{\boldsymbol{k}\sigma\boldsymbol{k}'\sigma'} = f_{-\boldsymbol{k}-\sigma-\boldsymbol{k}'-\sigma'}$. It is therefore useful to rewrite it as the sum of a symmetric and an antisymmetric contribution, $f_{\boldsymbol{k}\sigma\boldsymbol{k}'\sigma'} = f^s_{\boldsymbol{k}\boldsymbol{k}'} + \sigma\sigma' f^a_{\boldsymbol{k}\boldsymbol{k}'}$, where

$$f^s_{\boldsymbol{k}\boldsymbol{k}'} = \frac{1}{4}\sum_{\sigma\sigma'} f_{\boldsymbol{k}\sigma\boldsymbol{k}'\sigma'}$$
$$f^a_{\boldsymbol{k}\boldsymbol{k}'} = \frac{1}{4}\sum_{\sigma\sigma'} \sigma\sigma' f_{\boldsymbol{k}\sigma\boldsymbol{k}'\sigma'}.$$

Only the symmetric term contributes to the energy of the quasiparticles. Let us consider for simplicity a Fermi gas, the dispersion relation of which has spherical symmetry. Since quasiparticles are only well defined close to the Fermi level, we can assume that $|\boldsymbol{k}| \sim |\boldsymbol{k}'| \sim k_F$; therefore, $f^s_{\boldsymbol{k}\boldsymbol{k}'}$ and $f^a_{\boldsymbol{k}\boldsymbol{k}'}$ depend essentially only on the angle between $\boldsymbol{k}$ and $\boldsymbol{k}'$, while the dependence on the $\boldsymbol{k}$ vector's length is weak. Next, let us expand $f^s_{\boldsymbol{k}\boldsymbol{k}'}$ and $f^a_{\boldsymbol{k}\boldsymbol{k}'}$ in orthogonal Legendre polynomials $P_l(\cos\theta_{\boldsymbol{k}\boldsymbol{k}'})$, where $\theta_{\boldsymbol{k}\boldsymbol{k}'}$ is the angle between $\boldsymbol{k}$ and $\boldsymbol{k}'$. We have

$$f^{s/a}_{\boldsymbol{k}\boldsymbol{k}'} = \rho(\varepsilon_F) \sum_{l=0}^{\infty} F^{s/a}_l \; P_l(\cos\theta_{\boldsymbol{k}\boldsymbol{k}'}),$$

where F^s_l and F^a_l are dimensionless parameters. One can then show that the mass renormalization is given by

$$\frac{m^*}{m} = 1 + \frac{1}{3}F^s_1 > 1, \qquad F^s_1 > 0.$$

Quasiparticles are less compressible than particles, i.e., if κ is the compressibility

$$\frac{\kappa}{\kappa_0} = \frac{m^*}{m}\frac{1}{1+F^s_0} < 1, \qquad F^s_0 > 0.$$

They are, however, more spin-polarizable than electrons; correspondingly the system exhibits an enhanced Pauli susceptibility

$$\frac{\chi}{\chi^P} = \frac{m^*}{m}\frac{1}{1+F^a_0} > 1, \qquad F^a_0 < 0.$$

It has to be noticed that, because of the finite lifetime of quasiparticles and/or non-Fermi liquid phenomena of various nature, the temperature and energy regime in which the Fermi liquid behavior is observed can be very narrow. This happens, e.g., for heavy-fermion or Kondo systems; we will come back to this point again in the last part of the lecture.

2.1.3 Stoner instabilities

In the presence of the Coulomb interaction $U \neq 0$, finding the solution of the Hubbard model requires many-body techniques. Nevertheless, in the small-U limit, we can already learn a lot about magnetism from Hartree-Fock (HF) static mean-field theory. In the simplest version of the HF approximation we make the following substitution

$$H_U = U\sum_i n_{i\uparrow}n_{i\downarrow} \to H^{\rm HF}_U = U\sum_i \left[n_{i\uparrow}\langle n_{i\downarrow}\rangle + \langle n_{i\uparrow}\rangle n_{i\downarrow} - \langle n_{i\uparrow}\rangle\langle n_{i\downarrow}\rangle\right].$$

This approximation transforms the Coulomb two-particle interaction into an effective single-particle interaction. Let us search for a ferromagnetic solution and set therefore

$$\langle n_{i\sigma}\rangle = n_\sigma = \frac{n}{2} + \sigma m,$$

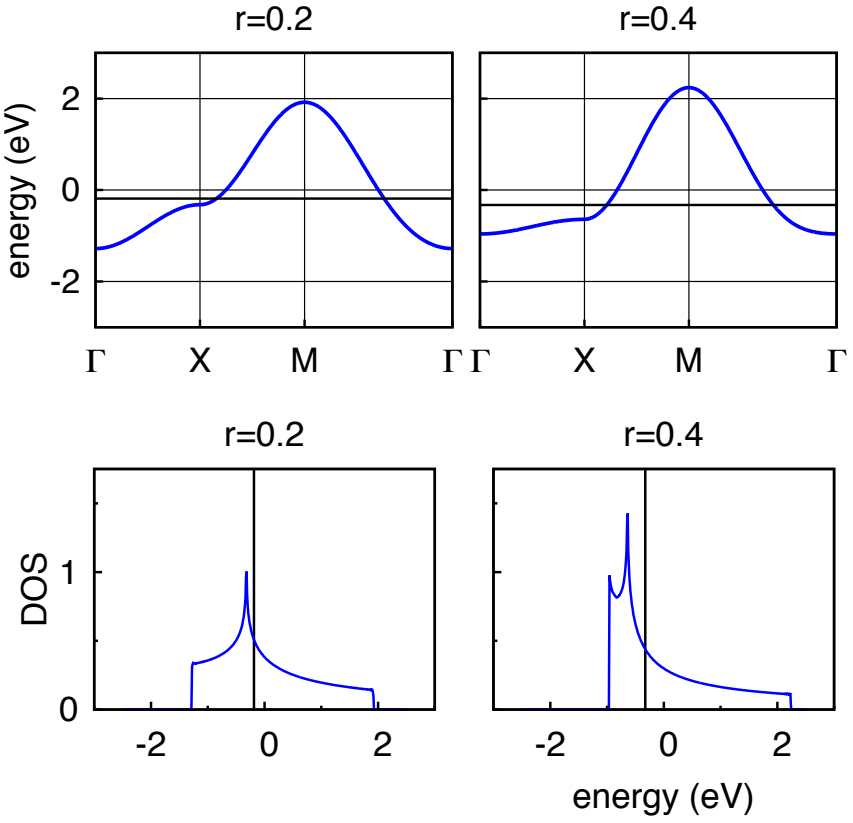

Fig. 5: *Top: Effect of $r = t'/t$ on the band structure of the two-dimensional tight-binding model. Black line: Fermi level at half filling. Bottom: corresponding density of states per spin.*

where $m = (n_\uparrow - n_\downarrow)/2$ and $n = n_\uparrow + n_\downarrow$. It is convenient to rewrite the mean-field Coulomb energy as in (10), i.e., as a function of m, n and S^i_z

$$H_U^{\rm HF} = U \sum_i \left[-2mS^i_z + m^2 + \frac{n^2}{4} \right] . \tag{13}$$

The solution of the problem defined by the Hamiltonian $H_0 + H_U^{\rm HF}$ amounts to the self-consistent solution of a non-interacting electron system with Bloch energies

$$\varepsilon^U_{\boldsymbol{k}\sigma} = \varepsilon_{\boldsymbol{k}} + n_{-\sigma}\, U = \varepsilon_{\boldsymbol{k}} + \frac{n}{2} U - \sigma m U \, .$$

In a magnetic field we additionally have to consider the Zeeman splitting. Thus

$$\varepsilon_{\boldsymbol{k}\sigma} = \varepsilon^U_{\boldsymbol{k}\sigma} + \frac{1}{2} g\mu_B h_z \sigma \, .$$

In the small-U limit and for $T \to 0$ the magnetization $M_z = -g\mu_B m$ is then given by

$$M_z \sim \chi^P(0) \left[h_z - \frac{2}{g\mu_B} U m \right] = \chi^P(0) \left[h_z + 2(g\mu_B)^{-2} U M_z \right] .$$

Solving for M_z we find the Stoner expression

$$\chi^S(\mathbf{0}; 0) = \frac{\chi^P(0)}{1 - 2\,(g\mu_B)^{-2}\, U \chi^P(0)} \, .$$

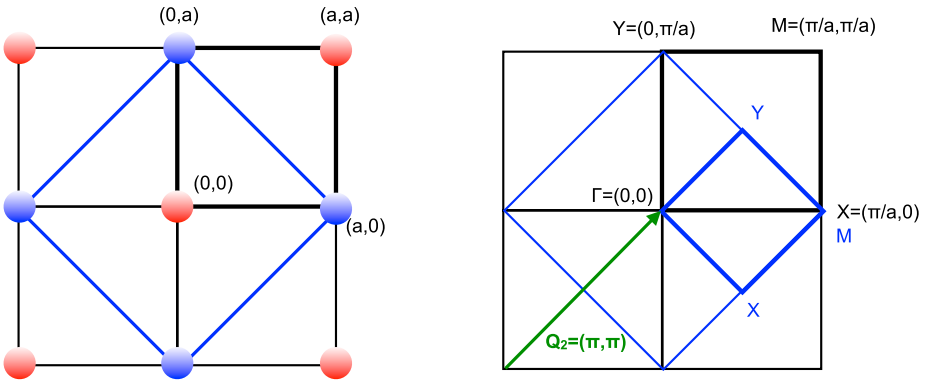

Fig. 6: *Doubling of the cell due to antiferromagnetic order and the corresponding folding of the Brillouin zone (BZ) for a two-dimensional hypercubic lattice. The antiferromagnetic* $\boldsymbol{Q}_2 = (\pi/a, \pi/a, 0)$ *vector is also shown.*

Thus with increasing U the $\boldsymbol{q} = \boldsymbol{0}$ static susceptibility increases and at the critical value

$$U_c = 2/\rho(\varepsilon_F)$$

diverges, i.e., even an infinitesimal magnetic field can produce a finite magnetization. This means that the ground state becomes unstable against ferromagnetic order.

Let us consider the case of the half-filled d-dimensional hypercubic lattice whose density of states is shown in Fig. 3. In three dimensions the DOS is flat around the Fermi level, e.g., $\rho(\varepsilon_F) \sim 2/W$ where W is the band width. For a flat DOS ferromagnetic instabilities are likely only when $U \sim W$, a rather large value of U, which typically also brings in strong-correlation effects not described by static mean-field theory. In two dimensions we have a rather different situation because a logarithmic Van-Hove singularity is exactly at the Fermi level (Fig. 3); a system with such a density of states is unstable towards ferromagnetism even for very small U. In real materials distortions or long-range interactions typically push the Van-Hove singularities away from the Fermi level. In HTSCs the electronic dispersion is modified as follows by the hopping t' between second-nearest neighbors

$$\varepsilon_{\boldsymbol{k}} = -2t[\cos(k_x a) + \cos(k_y a)] + 4t' \cos(k_x a) \cos(k_y a)\,.$$

As shown in Fig. 4, the parameter $r \sim t'/t$ ranges typically from ~ 0.15 to 0.4 [29]. Fig. 5 shows that with increasing r the Van-Hove singularity moves downwards in energy.

It is at this point natural to ask ourselves if ferromagnetism is the only possible instability. For a given system, magnetic instabilities with $\boldsymbol{q} \neq \boldsymbol{0}$ might be energetically favorable compared to ferromagnetism; an example of a finite-$\boldsymbol{q}$ instability is antiferromagnetism (see Fig. 6). To investigate finite-$\boldsymbol{q}$ instabilities we generalize the Stoner criterion. Let us consider a magnetic excitation characterized by the vector $\boldsymbol{q}$ commensurate with the reciprocal lattice. This magnetic superstructure defines a new lattice; the associated supercell includes $j = 1, \ldots, N_j$

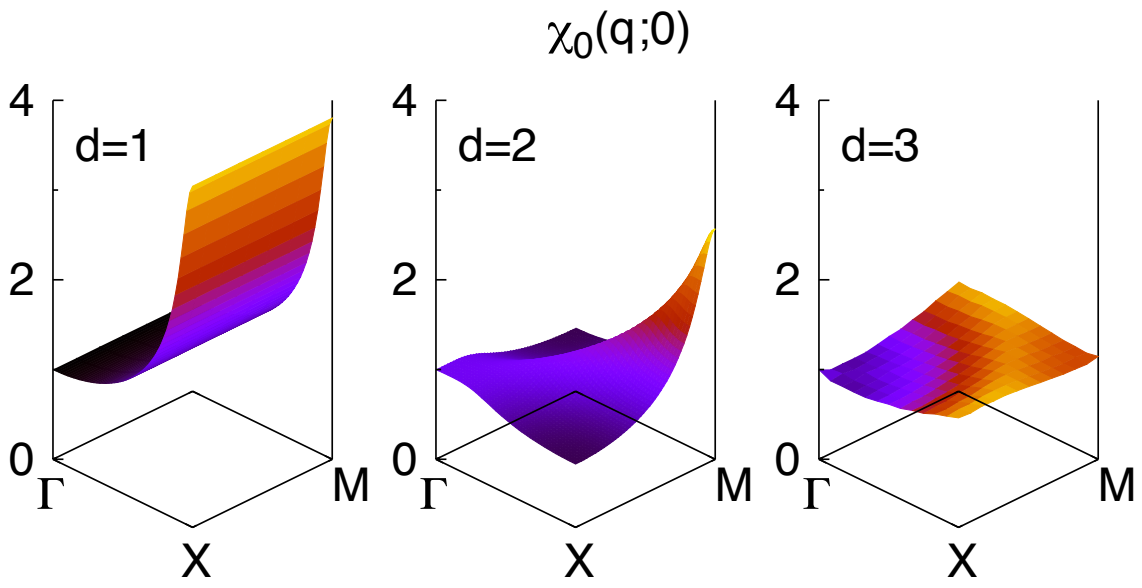

Fig. 7: *The ratio $\chi_0(\boldsymbol{q};0)/\chi_0(\boldsymbol{0};0)$ in the xy plane for a hypercubic lattice with $t = 0.4$ eV ($T \sim 230$ K) at half filling. From left to right: one, two, and three dimensions.*

magnetically inequivalent sites. We therefore define the quantities

$$S^i_z(\boldsymbol{q}) = \sum_j e^{i\boldsymbol{q}\cdot\boldsymbol{R}_j} S^{ji}_z,$$

$$\langle S^{ji}_z \rangle = m\cos(\boldsymbol{q}\cdot\boldsymbol{R}_j),$$

where j runs over the magnetically inequivalent sites $\{\boldsymbol{R}_j\}$ and i over the supercells in the lattice. In the presence of a magnetic field oscillating with vector $\boldsymbol{q}$ and pointing in the z direction, $\boldsymbol{h}_j = h_z\cos(\boldsymbol{q}\cdot\boldsymbol{R}_j)\hat{z}$, the mean-field Coulomb and Zeeman terms can be written as

$$H^{\rm HF}_U + H_Z = \sum_i \left[\frac{g\mu_B}{2}\left(h_z - \frac{2}{g\mu_B}mU\right)\left[S^i_z(\boldsymbol{q}) + S^i_z(-\boldsymbol{q})\right] + m^2 + \frac{n^2}{4}\right],$$

where m has to be determined self-consistently. This leads to the generalized Stoner formula

$$\chi^S(\boldsymbol{q};0) = \frac{1}{2}(g\mu_B)^2\frac{\chi_0(\boldsymbol{q};0)}{[1 - U\chi_0(\boldsymbol{q};0)]}, \tag{14}$$

$$\chi_0(\boldsymbol{q};0) = -\frac{1}{N_{\boldsymbol{k}}}\sum_{\boldsymbol{k}}\frac{n_{\boldsymbol{k}+\boldsymbol{q}} - n_{\boldsymbol{k}}}{\varepsilon_{\boldsymbol{k}+\boldsymbol{q}} - \varepsilon_{\boldsymbol{k}}}.$$

Expression (14) is also known as the RPA (acronym for random-phase approximation) susceptibility. For $\boldsymbol{q} = \boldsymbol{0}$ in the $T \to 0$ limit we recover the ferromagnetic RPA susceptibility with

$$\chi_0(\boldsymbol{0};0) = 2\,(g\mu_B)^{-2}\,\chi^P(0) \sim \frac{1}{2}\rho(\varepsilon_F)\,.$$

Figure 7 shows the non-interacting susceptibility in the xy plane for our d-dimensional hy-

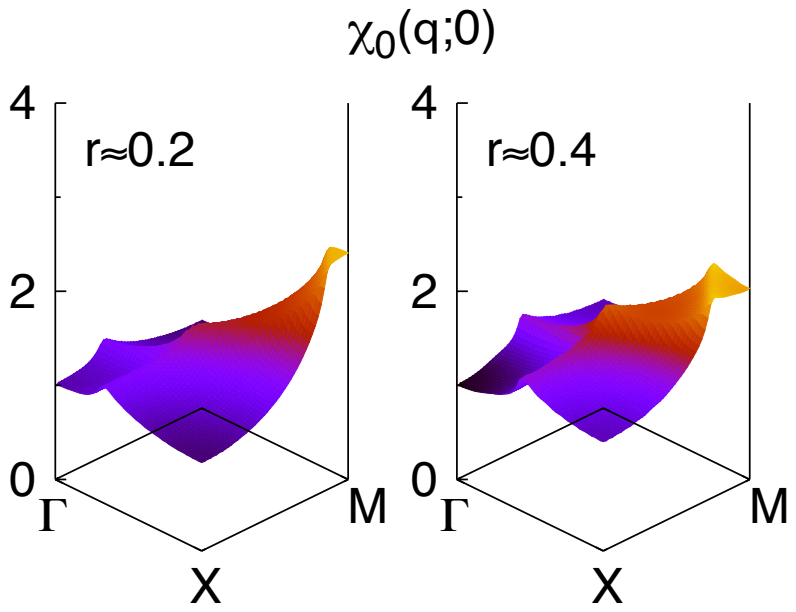

Fig. 8: *The ratio $\chi_0(\boldsymbol{q};0)/\chi_0(\boldsymbol{0};0)$ in the xy plane for the two-dimensional hypercubic lattice with $t = 0.4$ eV (230 K) at half filling. Left: $t' = 0.2t$. Right: $t' = 0.4t$.*

percubic lattice. The figure shows that in the one-dimensional case the susceptibility diverges at the antiferromagnetic vector $\boldsymbol{Q}_1 = (\pi/a, 0, 0)$; in two dimensions this happens at $\boldsymbol{Q}_2 = (\pi/a, \pi/a, 0)$; in three dimension at $\boldsymbol{Q}_3 = (\pi/a, \pi/a, \pi/a)$, not shown in the figure. The energy dispersion at these vectors exhibits the property of perfect nesting

$$\varepsilon_{\boldsymbol{k}+\boldsymbol{Q}_i} = -\varepsilon_{\boldsymbol{k}}\,.$$

Remarkably, the $T = 0$ non-interacting susceptibility $\chi_0(\boldsymbol{Q}_i;0)$ diverges logarithmically at the nesting vector unless the density of states is zero at the Fermi level ($\varepsilon \to 0$)

$$\chi_0(\boldsymbol{Q}_i;0) \propto \frac{1}{4}\int_{-\infty}^{\varepsilon_F=0} d\varepsilon\, \rho(\varepsilon)\frac{1}{\varepsilon} \to \infty\,.$$

Under these conditions an arbitrarily small U can cause a magnetic transition with magnetic vector $\boldsymbol{Q}_i$. In the two-dimensional case we have reached a similar conclusion for the $T = 0$ ferromagnetic ($\boldsymbol{q} = \boldsymbol{0}$) instability. The finite-temperature susceptibility $\chi_0(\boldsymbol{q};0)$, however, shows that the antiferromagnetic instability is the strongest (Fig. 7). Perfect nesting at $\boldsymbol{Q}_2$ is suppressed by $t' \neq 0$

$$\varepsilon_{\boldsymbol{k}+\boldsymbol{Q}_2} = -\varepsilon_{\boldsymbol{k}} + 8t'\cos(k_x a)\cos(k_y a).$$

Figure 8 shows how the susceptibility is modified by $t' \neq 0$ (half filling). The $\boldsymbol{Q}_2$ instability is important even for $t' \sim 0.4t$, but instabilities at incommensurate vectors around it are stronger. As a last remark it is important to notice that the RPA expression (14) depends on the filling only through the density of states, i.e., magnetic instabilities described by the Stoner formula can exist at *any* filling. This is very different from the case of the local-moment regime that we will discuss starting with the next section.

Ion			n	S	L	J	$^{2S+1}L_J$
V^{4+}	Ti^{3+}		$3d^1$	1/2	2	3/2	$^2D_{3/2}$
	V^{3+}		$3d^2$	1	3	2	$^3F_2$
	Cr^{3+}	V^{2+}	$3d^3$	3/2	3	3/2	$^4F_{3/2}$
	Mn^{3+}	Cr^{2+}	$3d^4$	2	2	0	$^5D_0$
	Fe^{3+}	Mn^{2+}	$3d^5$	5/2	0	5/2	$^6S_{5/2}$
		Fe^{2+}	$3d^6$	2	2	4	$^5D_4$
		Co^{2+}	$3d^7$	3/2	3	9/2	$^4F_{9/2}$
		Ni^{2+}	$3d^8$	1	3	4	$^3F_4$
		Cu^{2+}	$3d^9$	1/2	2	5/2	$^2D_{5/2}$

Table 1: *Quantum numbers of the ground-state multiplet for several transition-metal ions with partially filled d shells. In transition-metal oxides the angular momentum is typically quenched because of the crystal field and therefore only the total spin matters.*

2.2 Atomic limit

2.2.1 Paramagnetism of isolated ions

As we have seen, the ground-state multiplet of free ions with partially occupied shells can be determined via Hund's rules. In Tab. 1 and Tab. 2 we can find the values of the S, L, and J quantum numbers for the ground-state multiplets of the most common transition-metal and rare-earth ions. If $t = 0$ and $n = 1$, the Hubbard model (7) describes precisely a collection of idealized free ions with an incomplete shell. For such idealized ions the only possible multiplet is the one with quantum numbers $J = S = 1/2, L = 0$. In the presence of a uniform external magnetic field $h_z\hat{z}$ we can then obtain the magnetization per atom as

$$M_z = \langle M_z^i \rangle = -g\mu_B \frac{\mathrm{Tr}\,[e^{-g\mu_B h_z \beta S_z^i} S_z^i]}{\mathrm{Tr}\,[e^{-g\mu_B h_z \beta S_z^i}]} = g\mu_B S \tanh\left(g\mu_B h_z \beta S\right),$$

and thus

$$\frac{\partial M_z}{\partial h_z} = \left(g\mu_B S\right)^2 \frac{1}{k_B T}\ \left[1 - \tanh^2\left(g\mu_B h_z \beta S\right)\right].$$

The static uniform susceptibility is then given by the $h \to 0$ limit

$$\chi_{zz}(\mathbf{0}; 0) = \left(g\mu_B S\right)^2 \frac{1}{k_B T} = \frac{C_{1/2}}{T}, \tag{15}$$

where $C_{1/2}$ is the $S = 1/2$ Curie constant. If $S = 1/2$, the relation $S^2 = S(S+1)/3$ holds. Thus, for reasons that will become clear shortly, the Curie constant is typically expressed as

$$C_{1/2} = \frac{\left(g\mu_B\right)^2 S(S+1)}{3k_B}.$$

If the ions have ground-state total angular momentum J, we can calculate the susceptibility with the same technique, provided that we replace g with the Landé factor g_J

$$g_J = \frac{\langle JJ_zLS|(g\boldsymbol{S} + \boldsymbol{L}) \cdot \boldsymbol{J}|JJ_zLS\rangle}{\langle JJ_zLS|\boldsymbol{J} \cdot \boldsymbol{J}|JJ_zLS\rangle} \sim \frac{3}{2} + \frac{S(S+1) - L(L+1)}{2J(J+1)}$$

Ion	n	S	L	J	$^{2S+1}L_J$	g_J
Ce^{3+}	$4f^1$	1/2	3	5/2	$^2F_{5/2}$	6/7
Pr^{3+}	$4f^2$	1	5	4	$^3H_4$	4/5
Nd^{3+}	$4f^3$	3/2	6	9/2	$^4I_{9/2}$	8/11
Pm^{3+}	$4f^4$	2	6	4	$^5I_4$	3/5
Sm^{3+}	$4f^5$	5/2	5	5/2	$^6H_{5/2}$	2/7
Eu^{3+}	$4f^6$	3	3	0	$^7F_0$	0
Gd^{3+}	$4f^7$	7/2	0	7/2	$^8S_{7/2}$	2
Tb^{3+}	$4f^8$	3	3	6	$^7F_6$	3/2
Dy^{3+}	$4f^9$	5/2	5	15/2	$^6H_{15/2}$	4/3
Ho^{3+}	$4f^{10}$	2	6	8	$^5I_8$	5/4
Er^{3+}	$4f^{11}$	3/2	6	15/2	$^4I_{15/2}$	6/5
Tm^{3+}	$4f^{12}$	1	5	6	$^3H_6$	7/6
Yb^{3+}	$4f^{13}$	1/2	3	7/2	$^2F_{7/2}$	8/7

Table 2: *Quantum numbers of the ground-state multiplet for rare-earth ions with partially filled f shells and corresponding g_J factor. In $4f$ materials the crystal field is typically small; thus the ground-state multiplet is to first approximation close to that of the corresponding free ion.*

and calculate the thermal average of the magnetization $\boldsymbol{M} = -g_J\mu_B\boldsymbol{J}$, accounting for the $2J+1$ degeneracy of the multiplet. The result is

$$M_z = \langle M_z^i \rangle = g_J\mu_B J \; B_J\left(g_J\mu_B h_z \beta J\right),$$

where $B_J(x)$ is the Brillouin function

$$B_J(x) = \frac{2J+1}{2J}\coth\left(\frac{2J+1}{2J}x\right) - \frac{1}{2J}\coth\left(\frac{1}{2J}x\right).$$

In the low-temperature ($x \to \infty$) limit $B_J(x) \sim 1$, and thus the magnetization approaches its saturation value in which all atoms are in the ground state

$$M_z \sim g_J\mu_B J \equiv M_0\,.$$

In the high-temperature ($x \to 0$) limit

$$B_J(x) \sim x\,\frac{J+1}{3J}\left[1 - \frac{2J^2+2J+1}{30J^2}x^2\right],$$

and thus the susceptibility exhibits the Curie high-temperature behavior

$$\chi_{zz}(\mathbf{0};0) \sim \frac{C_J}{T} = \frac{\mu_J^2}{3k_BT}\,,$$

where the generalized Curie constant is

$$C_J = \frac{(g_J\mu_B)^2 J(J+1)}{3k_B}$$

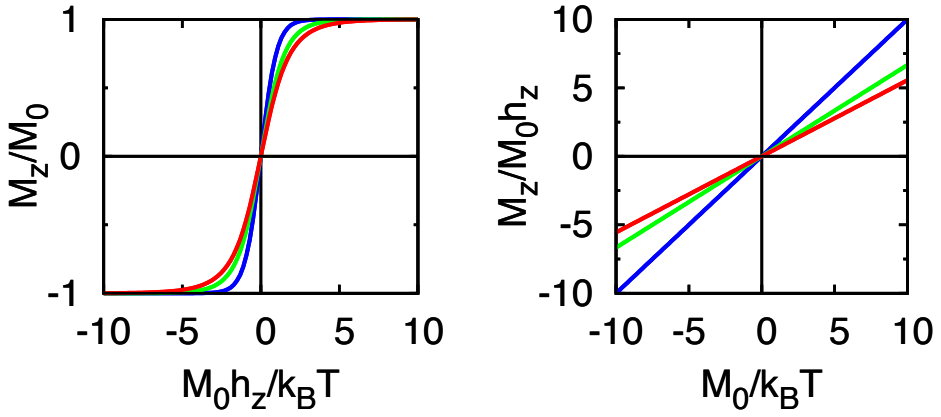

Fig. 9: *Left:* $M_z/M_0 = B_J(x)$ *as a function of* $x = h_z M_0/k_BT$. *The different lines correspond to* $J = 1/2$ *(blue),* $J = 1$ *(green) and* $J = 3/2$ *(red). Right: The ratio* M_z/M_0h_z *for finite magnetic field in the small* x *limit; the slope is* $(J+1)/3J$.

and where $\mu_J = g_J\mu_B\sqrt{J(J+1)}$ is the total magnetic moment. Correspondingly, the susceptibility decreases as $1/T$ with increasing T (Fig. 9). We have thus the three limiting cases

$$\chi_{zz}(\mathbf{0};0) \sim \begin{cases} 0 & k_BT/|M_0|h_z \to 0 \\ C_J/T & |M_0|h_z/k_BT \to 0 \\ C_J/T & h_z \to 0 \end{cases} .$$

Remarkably, the $T \to 0$ and $h_z \to 0$ limit cannot be interchanged. If h_z is finite the susceptibility goes to zero in the $T \to 0$ limit; if we instead perform the $h_z \to 0$ limit first it diverges with the Curie form $1/T$. The point $h_z = T = 0$ is a critical point in the phase space.
Let us return to the $S = 1/2$ case, i.e., the one relevant for the Hubbard model. It is interesting to calculate the inter-site spin correlation function $\mathcal{S}_{i,i'}$

$$\mathcal{S}_{i,i'} = \langle(\boldsymbol{S}_i - \langle\boldsymbol{S}_i\rangle)\cdot(\boldsymbol{S}_{i'} - \langle\boldsymbol{S}_{i'}\rangle)\rangle = \langle\boldsymbol{S}_i\cdot\boldsymbol{S}_{i'}\rangle - \langle\boldsymbol{S}_i\rangle\cdot\langle\boldsymbol{S}_{i'}\rangle\,.$$

We express $\langle\boldsymbol{S}_i\cdot\boldsymbol{S}_{i'}\rangle$ in the form $[S(S+1)-S_i(S_i+1)-S_{i'}(S_{i'}+1)]/2$, where $S_i = S_{i'} = 1/2$ and $\boldsymbol{S} = \boldsymbol{S}_i + \boldsymbol{S}_{i'}$ is the total spin. Then, since in the absence of a magnetic field $\langle\boldsymbol{S}_i\rangle = \langle\boldsymbol{S}_{i'}\rangle = 0$,

$$\mathcal{S}_{i,i'} = [S(S+1) - 3/2]/2 = \begin{cases} 1/4 & S = 1 \\ -3/4 & S = 0 \end{cases} .$$

The ideal paramagnetic state is however characterized by uncorrelated sites. Hence

$$\mathcal{S}_{i,i'} = \langle\boldsymbol{S}_i\cdot\boldsymbol{S}_{i'}\rangle \sim \begin{cases} \langle\boldsymbol{S}_i\rangle\cdot\langle\boldsymbol{S}_{i'}\rangle & \sim 0 \quad i \neq i' \\ \langle\boldsymbol{S}_i\cdot\boldsymbol{S}_i\rangle & = 3/4 \quad i = i' \end{cases} . \tag{16}$$

The (ideal) paramagnetic phase is thus quite different from a spatially disordered state, i.e., a situation in which each ion has a spin oriented in a given direction but spin orientations are randomly distributed. In the latter case, in general, $\langle\boldsymbol{S}^i\cdot\boldsymbol{S}^{i'}\rangle \neq 0$ for $i' \neq i$, even if, e.g., the sum of $\langle S_z^i\cdot S_z^{i'}\rangle$ over all sites i' with $i' \neq i$ is zero

$$\sum_{i'\neq i}\langle S_z^i\cdot S_z^{i'}\rangle \sim 0\,.$$

The high-temperature static susceptibility can be obtained from the correlation function Eq. (16) using the *fluctuation-dissipation theorem* and the Kramers-Kronig relations (see Appendix). The result is

$$\chi_{zz}(\boldsymbol{q};0) \sim \frac{(g\mu_B)^2}{k_B T} \sum_j \mathcal{S}_{zz}^{i,i+j} e^{i\boldsymbol{q}\cdot(\boldsymbol{R}_i - \boldsymbol{R}_{i+j})} = \chi_{zz}^i(T) = \frac{M_0^2}{k_B T} = \frac{C_{1/2}}{T}. \tag{17}$$

This shows that $\chi_{zz}(\boldsymbol{q};0)$ is $\boldsymbol{q}$-independent and coincides with the local susceptibility $\chi_{zz}^i(T)$

$$\chi_{zz}(\mathbf{0};0) = \lim_{h_z \to 0} \frac{\partial M_z}{\partial h_z} = \chi_{zz}^i(T)\,.$$

How can the spin susceptibility (17) be obtained directly from Hamiltonian (10), the atomic limit of the Hubbard model? To calculate it we can use, e.g., the imaginary-time and Matsubara-frequency formalism (see Appendix). Alternatively at high temperatures we can obtain it from the correlation function as we have just seen. The energies of the four atomic states are given by (9) and, at half filling, the chemical potential is $\mu = \varepsilon_d + U/2$. Therefore

$$\chi_{zz}(\mathbf{0};0) \sim \frac{(g\mu_B)^2}{k_B T} \left(\frac{\mathrm{Tr}\left[e^{-\beta(H_i - \mu N_i)} \ (S_z^i)^2\right]}{\mathrm{Tr}\left[e^{-\beta(H_i-\mu N_i)}\right]} - \left[\frac{\mathrm{Tr}\left[e^{-\beta(H_i-\mu N_i)} \ S_z^i\right]}{\mathrm{Tr}\left[e^{-\beta(H_i-\mu N_i)}\right]}\right]^2 \right) = \frac{C_{1/2}}{T} \frac{e^{\beta U/2}}{1+e^{\beta U/2}}\,.$$

Thus, the susceptibility depends on the energy scale

$$U = E(N_i+1) + E(N_i-1) - 2E(N_i).$$

If we perform the limit $U \to \infty$, we effectively eliminate doubly occupied and empty states. In this limit, we recover the expression that we found for the spin $S = 1/2$ model, Eq. (17). This is a trivial example of downfolding, in which the low-energy and high-energy sector are decoupled in the Hamiltonian from the start. In the large-U limit the high-energy states are integrated out leaving the system in a magnetic $S = 1/2$ state.

2.2.2 Larmor diamagnetism and Van Vleck paramagnetism

For ions with $J = 0$ the ground-state multiplet, in short $|0\rangle$, is non-degenerate and the linear correction to the ground-state total energy due to the Zeeman term is zero. Remarkably, for open-shell ions the magnetization nevertheless remains finite because of higher-order corrections. At second order there are two contributions for the ground state. The first is the Van-Vleck term

$$M_z^{\mathrm{VV}} = 2h_z\mu_B^2 \sum_I \frac{|\langle 0|(L_z + gS_z)|I\rangle|^2}{E_I - E_0},$$

where E_I is the energy of the excited state $|I\rangle$ and E_0 the energy of the ground-state multiplet. The Van Vleck term is weakly temperature-dependent and typically small. The second term is the diamagnetic Larmor contribution

$$M_z^{\mathrm{L}} = -\frac{1}{4} h_z \langle 0| \sum_i (x_i^2 + y_i^2)|0\rangle.$$

The Larmor and Van Vleck terms have opposite signs and typically compete with each other.

2.3 Strong-correlation limit

2.3.1 From the Hubbard model to the Heisenberg model

In the large-U limit and at half filling we can map the Hubbard model onto an effective Heisenberg model. In this section we solve the latter using static mean-field theory. In the mean-field approximation we replace the Heisenberg Hamiltonian (11) with

$$H_S^{\rm MF} = \frac{1}{2}\Gamma \sum_{\langle ii'\rangle} \left[\boldsymbol{S}_i \cdot \langle \boldsymbol{S}_{i'}\rangle + \langle \boldsymbol{S}_i\rangle \cdot \boldsymbol{S}_{i'} - \langle \boldsymbol{S}_i\rangle \cdot \langle \boldsymbol{S}_{i'}\rangle - \frac{1}{4} n_i n_{i'} \right].$$

In the presence of an external magnetic field $\boldsymbol{h}$ we add the Zeeman term and have in total

$$\begin{aligned} H &= g\mu_B \sum_i \left[\boldsymbol{S}_i \cdot (\boldsymbol{h} + \boldsymbol{h}_i^m) + \text{const.} \right] , \\ \boldsymbol{h}_i^m &= n_{\langle ii'\rangle} \Gamma \langle \boldsymbol{S}_{i'}\rangle / g\mu_B \, , \end{aligned}$$

where $n_{\langle ii'\rangle}$ is the number of first nearest neighbors and $\boldsymbol{h}_i^m$ is the molecular field at site i. We define the quantization axis z as the direction of the external magnetic field, $\boldsymbol{h} = h_z \hat{z}$, and assume that $\hat{z}$ is also the direction of the molecular field, $\boldsymbol{h}_i^m = \Delta h_z^i \hat{z}$. Since $\Gamma > 0$ and hypercubic lattices are bipartite, the likely magnetic order is two-sublattice antiferromagnetism. Thus we set $M_z^A = -g\mu_B \langle S_z^i\rangle$, $M_z^B = -g\mu_B \langle S_z^{i'}\rangle$, where A and B are the two sublattices, $i \in A$ and $i' \in B$. In the absence of an external magnetic field, the total magnetization per formula unit, $M_z = (M_z^B + M_z^A)/2$, vanishes in the antiferromagnetic state ($M_z^B = -M_z^A$). We define therefore as the order parameter $\sigma_m = 2m = (M_z^B - M_z^A)/2M_0$, which is zero only above the critical temperature for antiferromagnetic order. We then calculate the magnetization for each sublattice and find the system of coupled equations

$$\left\{ \begin{array}{rcl} M_z^A/M_0 &=& B_{1/2}\left[M_0(h_z + \Delta h_z^A)\beta\right] \\ M_z^B/M_0 &=& B_{1/2}\left[M_0(h_z + \Delta h_z^B)\beta\right] \end{array} \right. , \tag{18}$$

where

$$\left\{ \begin{array}{rl} \Delta h_z^A = & -(M_z^B/M_0)\, S^2 \Gamma n_{\langle ii'\rangle}/M_0 \\ \Delta h_z^B = & -(M_z^A/M_0)\, S^2 \Gamma n_{\langle ii'\rangle}/M_0 \end{array} \right. .$$

For $h_z = 0$ the system (18) can be reduced to the single equation

$$\sigma_m = B_{1/2}\Big[\sigma_m S^2 \Gamma n_{\langle ii'\rangle}\beta\Big]. \tag{19}$$

This equation always has the trivial solution $\sigma_m = 0$. Figure 10 shows that, for small-enough temperatures it also has a non-trivial solution $\sigma_m \neq 0$. The order parameter σ_m equals ± 1 at zero temperature, and its absolute value decreases with increasing temperature. It becomes zero for $T \geq T_{\rm N}$ with

$$k_B T_{\rm N} = \frac{S(S+1)}{3} n_{\langle ii'\rangle} \Gamma.$$

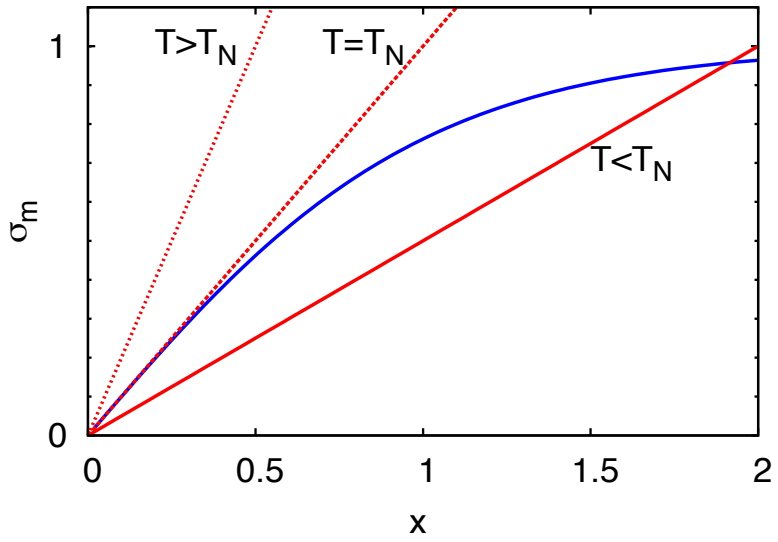

Fig. 10: *The self-consistent solution of Eq. (20) for $\sigma_m \geq 0$. The blue line shows the right-hand side of the equation, the Brillouin function $B_{1/2}(x)$, with $x = \sigma_m T_{\rm N}/T$. The red lines show the left-hand side of the equation, $\sigma_m(x) = \alpha\, x$, with $\alpha = T/T_{\rm N}$; the three different curves correspond to representative $T/T_{\rm N}$ values.*

If $T \sim T_{\rm N}$, we can find the non-trivial solution by first rewriting (19) as

$$\sigma_m = B_{1/2}\left[\frac{T_{\rm N}}{T}\sigma_m\right]. \tag{20}$$

The inverse of this equation yields $T/T_{\rm N}$ as a function of σ_m

$$\frac{T}{T_{\rm N}} = \frac{\sigma_m}{B^{-1}_{1/2}\left[\sigma_m\right]}.$$

If $T \sim T_{\rm N}$, the parameter σ_m is small. We then expand the right-hand-side in powers of σ_m

$$\frac{\sigma_m}{B^{-1}_{1/2}(\sigma_m)} \sim \frac{\sigma_m}{\sigma_m + \sigma_m^3/3 + \ldots} \sim 1 - \sigma_m^2/3 + \ldots.$$

This leads to the following expression

$$\sigma_m = \sqrt{3}\left(1 - \frac{T}{T_{\rm N}}\right)^{1/2},$$

which shows that the order parameter has a discontinuous temperature derivative at $T = T_{\rm N}$.
It is interesting to derive the expression of the static uniform susceptibility. For this we go back to the system of equations (18) and calculate from it the total magnetization M_z. In the weak magnetic field limit, $M_z^A \sim -\sigma_m M_0 + \chi_{zz}(\mathbf{0};0)h_z$, and $M_z^B \sim \sigma_m M_0 + \chi_{zz}(\mathbf{0};0)h_z$. Then, by performing the first derivative of M_z with respect to h_z in the $h_z \to 0$ limit, we obtain

$$\chi_{zz}(\mathbf{0};0) = \frac{C_{1/2}(1-\sigma_m^2)}{T + (1-\sigma_m^2)T_{\rm N}}.$$

The uniform susceptibility vanishes at $T = 0$ and reaches the maximum at $T = T_{\rm N}$, where it takes the value $C_{1/2}/2T_{\rm N}$. In the high-temperature regime $\sigma_m = 0$ and

$$\chi_{zz}(\mathbf{0};0) \sim \frac{C_{1/2}}{T + T_{\rm N}},$$

which is *smaller* than the susceptibility of free $S = 1/2$ magnetic ions.
The magnetic linear response is quite different if we apply an external field $\boldsymbol{h}_\perp$ perpendicular to the spins in the antiferromagnetic lattice. The associated perpendicular magnetization is

$$M_\perp \sim M_0 \frac{\sigma_m(g\mu_B h_\perp)}{\sqrt{(g\mu_B h_\perp)^2 + (4\sigma_m)^2 (k_B T_{\rm N})^2}},$$

and therefore the perpendicular susceptibility is temperature-independent for $T \leq T_{\rm N}$

$$\chi_\perp(\mathbf{0};0) = \lim_{h_\perp \to 0} \frac{dM_\perp}{dh_\perp} = \frac{C_{1/2}}{2T_{\rm N}}.$$

Hence, for $T < T_{\rm N}$ the susceptibility is anisotropic, $\chi_{zz}(\mathbf{0};0) = \chi_\parallel(\mathbf{0};0) \neq \chi_\perp(\mathbf{0};0)$; at absolute zero $\chi_\parallel(\mathbf{0};0)$ vanishes, but the response to $\boldsymbol{h}_\perp$ remains strong. For $T > T_{\rm N}$ the order parameter is zero and the susceptibility isotropic, $\chi_\parallel(\mathbf{0};0) = \chi_\perp(\mathbf{0};0)$.
We have up to now considered antiferromagnetic order only. What about other magnetic instabilities? Let us consider first ferromagnetic order. For a ferromagnetic spin arrangement, by repeating the calculation, we find

$$\chi_{zz}(\mathbf{0};0) = \frac{C_{1/2}(1-\sigma_m^2)}{T - (1-\sigma_m^2)T_{\rm C}},$$

where $T_C = -S(S+1)n_{\langle ii'\rangle}\Gamma/3k_B$ is, if the exchange coupling Γ is negative, the critical temperature for ferromagnetic order. Then, in contrast to the antiferromagnetic case, the high-temperature uniform susceptibility is *larger* than that of free $S = 1/2$ magnetic ions.
For a generic magnetic structure characterized by a vector $\boldsymbol{q}$ and a supercell with $j = 1, \ldots, N_j$ magnetically inequivalent sites we make the ansatz

$$\langle M_z^{ji} \rangle = -\sigma_m M_0 \cos(\boldsymbol{q}\cdot\boldsymbol{R}_j) = -g\mu_B\, m\, \cos(\boldsymbol{q}\cdot\boldsymbol{R}_j)\,,$$

where σ_m is again the order parameter, i identifies the supercell, and $\boldsymbol{R}_j$ the position of the j-th inequivalent site. We consider a magnetic field rotating with the same $\boldsymbol{q}$ vector. By using the static mean-field approach we then find

$$k_B T_{\boldsymbol{q}} = \frac{S(S+1)}{3}\Gamma_{\boldsymbol{q}}, \quad \Gamma_{\boldsymbol{q}} = -\sum_{ij\neq 0} \Gamma^{00,ij} e^{i\boldsymbol{q}\cdot(\boldsymbol{T}_i + \boldsymbol{R}_j)}, \tag{21}$$

where $\Gamma^{00,ij}$ is the exchange coupling between the spin at the origin and the spin at site $\boldsymbol{T}_i + \boldsymbol{R}_j$ (ij in short); $\{\boldsymbol{R}_j\}$ are vectors inside a supercell and $\{\boldsymbol{T}_i\}$ are lattice vectors. In our example, $T_{\mathbf{0}} = T_{\rm C}$ and $T_{\boldsymbol{q}_{\rm AF}} = T_{\rm N} = -T_{\rm C}$. Thus we have

$$\chi_{zz}(\boldsymbol{q};0) = \frac{C_{1/2}(1-\sigma_m^2)}{T - (1-\sigma_m^2)T_{\boldsymbol{q}}}, \tag{22}$$

which diverges at $T = T_{\boldsymbol{q}}$. The susceptibility $\chi_{zz}(\boldsymbol{q}; 0)$ reflects the spatial extent of correlations, i.e., the *correlation length* ξ; the divergence of the susceptibility at $T_{\boldsymbol{q}}$ is closely related to the divergence of ξ. To see this we calculate ξ for a hypercubic three-dimensional lattice, assuming that the system has only one instability with vector $\boldsymbol{Q}$. First we expand Eq. (21) around $\boldsymbol{Q}$ obtaining $T_{\boldsymbol{q}} \sim T_{\boldsymbol{Q}} + \alpha(\boldsymbol{q} - \boldsymbol{Q})^2 + \ldots$, and then we calculate $\chi_{zz}^{00,ji}$, the Fourier transform of Eq. (22). We find that $\chi_{zz}^{00,ji}$ decays exponentially with $r = |\boldsymbol{T}_i + \boldsymbol{R}_j|$, i.e., $\chi_{zz}^{00,ji} \propto e^{-r/\xi}/r$. The range of the correlations is $\xi \propto [T_{\boldsymbol{Q}}/(T - T_{\boldsymbol{Q}})]^{1/2}$, which becomes infinite at $T = T_{\boldsymbol{Q}}$. It is important to notice that in principle there can be instabilities at any $\boldsymbol{q}$ vector, i.e., $\boldsymbol{q}$ need not be commensurate with reciprocal lattice vectors. The value of $\boldsymbol{q}$ for which $T_{\boldsymbol{q}}$ is the largest determines (within static mean-field theory) the type of magnetic order that is realized. The antiferromagnetic structure in Fig. 6 corresponds to $\boldsymbol{q}_{\rm AF} = \boldsymbol{Q}_2 = (\pi/a, \pi/a, 0)$.
In real systems the spin S is typically replaced by an *effective magnetic moment*, $\mu_{\rm eff}$, and therefore $C_{1/2} \to C_{\rm eff} = \mu_{\rm eff}^2/3k_B$. It follows that $\mu_{\rm eff}$ is the value of the product $3k_BT\chi_{zz}(\boldsymbol{q}; 0)$ in the high-temperature limit (here $T \gg T_{\boldsymbol{q}}$). The actual value of $\mu_{\rm eff}$ depends, as we have discussed in the introduction, on the Coulomb interaction, the spin-orbit coupling and the crystal field. In addition, the effective moment can be screened by many-body effects, as happens for Kondo impurities; we will discuss the latter case in the last section.

2.3.2 The Hartree-Fock approximation

We have seen that Hartree-Fock (HF) mean-field theory yields Stoner magnetic instabilities in the weak-coupling limit. Can it also describe magnetism in the local-moment regime ($t/U \ll 1$)? Let us focus on the half-filled two-dimensional Hubbard model for a square lattice, and let us analyze two possible magnetically ordered states, the ferro- and the antiferromagnetic state. If we are only interested in the ferromagnetic or the paramagnetic solution, the HF approximation of the Coulomb term in the Hubbard model is given by Eq. (13). Thus the Hamiltonian is $H = H_d + H_T + H_U^{\rm HF}$ with $H_U^{\rm HF} = U\sum_i[-2mS_z^i + m^2 + \frac{1}{4}n^2]$. For periodic systems it is convenient to write H in $\boldsymbol{k}$ space. We then adopt as one-electron basis the Bloch states

$$\Psi_{\boldsymbol{k}\sigma}(\boldsymbol{r}) = \frac{1}{\sqrt{N_s}} \sum_i e^{i\boldsymbol{k}\cdot\boldsymbol{T}_i}\, \Psi_{i\sigma}(\boldsymbol{r}),$$

where $\Psi_{i\sigma}(\boldsymbol{r})$ is a Wannier function with spin σ, $\boldsymbol{T}_i$ a lattice vector, and N_s the number of lattice sites. The term $H_U^{\rm HF}$ depends on the spin operator S_z^i, which can be written in $\boldsymbol{k}$ space as

$$S_z^i = \frac{1}{N_{\boldsymbol{k}}} \sum_{\boldsymbol{k}\boldsymbol{k}'} e^{i(\boldsymbol{k}-\boldsymbol{k}')\cdot\boldsymbol{T}_i} \underbrace{\frac{1}{2}\sum_\sigma \sigma c_{\boldsymbol{k}\sigma}^\dagger c_{\boldsymbol{k}'\sigma}}_{S_z(\boldsymbol{k},\boldsymbol{k}')} = \frac{1}{N_{\boldsymbol{k}}} \sum_{\boldsymbol{k}\boldsymbol{k}'} e^{i(\boldsymbol{k}-\boldsymbol{k}')\cdot\boldsymbol{T}_i} S_z(\boldsymbol{k}, \boldsymbol{k}').$$

The term $H_U^{\rm HF}$ has the same periodicity as the lattice and does not couple states with different $\boldsymbol{k}$ vectors. Thus only $S_z(\boldsymbol{k}, \boldsymbol{k})$ contributes, and the Hamiltonian can be written as

$$H = \sum_\sigma \sum_{\boldsymbol{k}} \varepsilon_{\boldsymbol{k}} n_{\boldsymbol{k}\sigma} + \underbrace{U \sum_{\boldsymbol{k}} \left[-2m\, S_z(\boldsymbol{k}, \boldsymbol{k}) + m^2 + \frac{n^2}{4}\right]}_{H_U^{\rm HF} = U\sum_i[-2mS_z^i + m^2 + \frac{1}{4}n^2]},$$

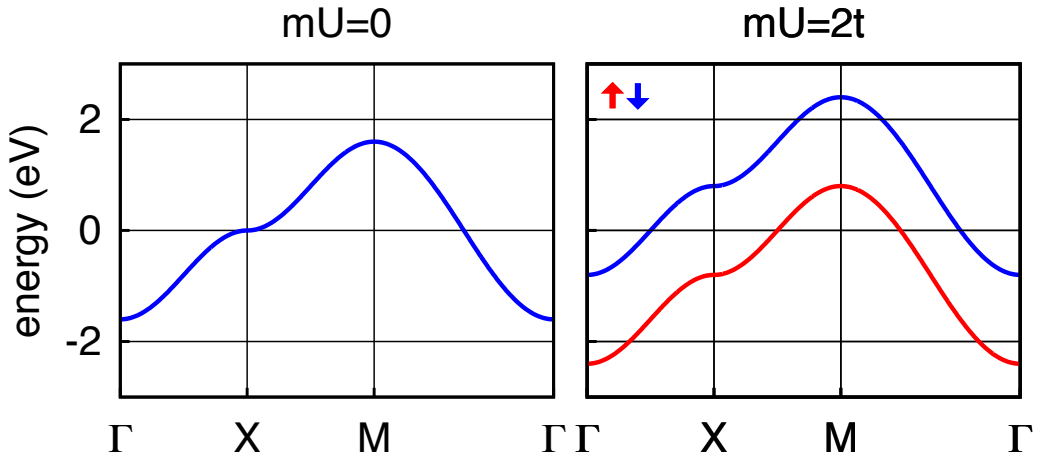

Fig. 11: *Ferromagnetism in Hartree-Fock. The chemical potential is taken as the energy zero.*

where $m = (n_\uparrow - n_\downarrow)/2$ and $n = 1$; for simplicity we set $\varepsilon_d = 0$. The HF correction splits the bands with opposite spin, leading to new one-electron eigenvalues, $\varepsilon_{\boldsymbol{k}\sigma} = \varepsilon_{\boldsymbol{k}} + \frac{1}{2}U - \sigma U m$; the chemical potential is $\mu = U/2$. The separation between $\varepsilon_{\boldsymbol{k}\uparrow} - \mu$ and $\varepsilon_{\boldsymbol{k}\downarrow} - \mu$ is $2mU$, as can be seen in Fig. 11. The system remains metallic for U smaller than the bandwidth W. In the small-t/U limit and at half filling we can assume that the system is a ferromagnetic insulator and $m = 1/2$. The total energy of the ground state is then

$$E_{\rm F} = \frac{1}{N_{\boldsymbol{k}}} \sum_{\boldsymbol{k}} \left[\varepsilon_{\boldsymbol{k}\sigma} - \mu\right] = \frac{1}{N_{\boldsymbol{k}}} \sum_{\boldsymbol{k}} \left[\varepsilon_{\boldsymbol{k}} - \frac{1}{2}U\right] = -\frac{1}{2}U.$$

Let us now describe the same periodic lattice via a supercell which allows for a two-sublattice antiferromagnetic solution; this supercell is shown in Fig. 6. We rewrite the Bloch states of the original lattice as

$$\Psi_{\boldsymbol{k}\sigma}(\boldsymbol{r}) = \frac{1}{\sqrt{2}}\left[\Psi^A_{\boldsymbol{k}\sigma}(\boldsymbol{r}) + \Psi^B_{\boldsymbol{k}\sigma}(\boldsymbol{r})\right], \qquad \Psi^\alpha_{\boldsymbol{k}\sigma}(\boldsymbol{r}) = \frac{1}{\sqrt{N_{s_\alpha}}} \sum_{i_\alpha} e^{i\boldsymbol{T}^\alpha_i \cdot \boldsymbol{k}}\, \Psi_{i_\alpha\sigma}(\boldsymbol{r}).$$

Here A and B are the two sublattices with opposite spins and $\boldsymbol{T}^A_i$ and $\boldsymbol{T}^B_i$ are their lattice vectors; $\alpha = A, B$. We take as one-electron basis the two Bloch functions $\Psi_{\boldsymbol{k}\sigma}$ and $\Psi_{\boldsymbol{k}+\boldsymbol{Q}_2\sigma}$, where $\boldsymbol{Q}_2 = (\pi/a, \pi/a, 0)$ is the vector associated with the antiferromagnetic instability and the corresponding folding of the Brillouin zone, also shown in Fig. 6. Then, in the HF approximation, the Coulomb interaction is given by

$$H_U^{\rm HF} = \sum_{i\in A}\left[-2mS^i_z + m^2 + \frac{n^2}{4}\right] + \sum_{i\in B}\left[+2mS^i_z + m^2 + \frac{n^2}{4}\right].$$

This interaction couples Bloch states with $\boldsymbol{k}$ vectors made equivalent by the folding of the Brillouin zone. Thus the HF Hamiltonian takes the form

$$H = \sum_{\boldsymbol{k}}\sum_{\sigma} \varepsilon_{\boldsymbol{k}} n_{\boldsymbol{k}\sigma} + \sum_{\boldsymbol{k}}\sum_{\sigma} \varepsilon_{\boldsymbol{k}+\boldsymbol{Q}_2} n_{\boldsymbol{k}+\boldsymbol{Q}_2\sigma} + \underbrace{U\sum_{\boldsymbol{k}}\left[-2m\, S_z(\boldsymbol{k}, \boldsymbol{k}+\boldsymbol{Q}_2) + 2m^2 + 2\frac{n^2}{4}\right]}_{\text{static mean-field correction } H_U^{\rm HF}}.$$

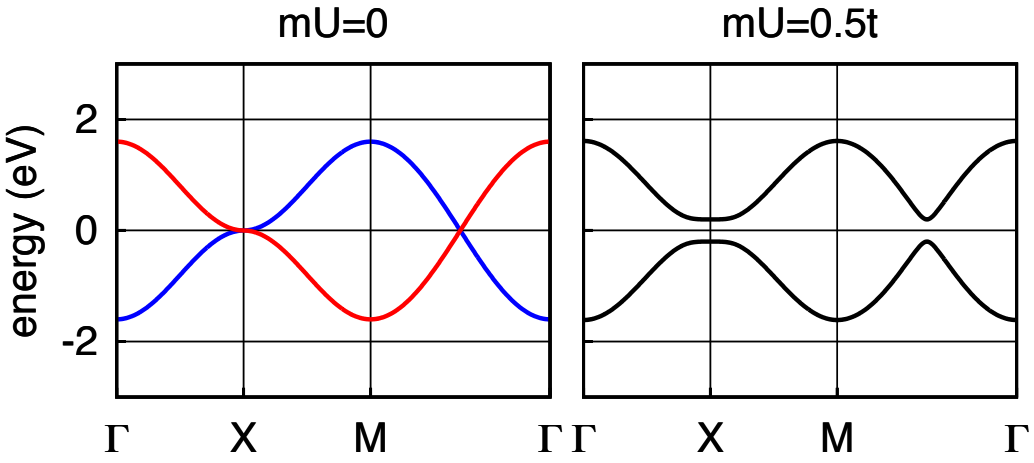

Fig. 12: *Antiferromagnetism in Hartree-Fock. The chemical potential is taken as the energy zero. Blue:* $\varepsilon_{\boldsymbol{k}}$*. Red:* $\varepsilon_{\boldsymbol{k}+\boldsymbol{Q}_2} = -\varepsilon_{\boldsymbol{k}}$*. The high-symmetry lines are those of the large BZ in Fig. 6.*

The sum over $\boldsymbol{k}$ is restricted to the Brillouin zone of the antiferromagnetic lattice. We find the two-fold degenerate eigenvalues

$$\varepsilon_{\boldsymbol{k}\pm} - \mu = \frac{1}{2}(\varepsilon_{\boldsymbol{k}} + \varepsilon_{\boldsymbol{k}+\boldsymbol{Q}_2}) \pm \frac{1}{2}\sqrt{(\varepsilon_{\boldsymbol{k}} - \varepsilon_{\boldsymbol{k}+\boldsymbol{Q}_2})^2 + 4(mU)^2}. \tag{23}$$

A gap opens where the bands $\varepsilon_{\boldsymbol{k}}$ and $\varepsilon_{\boldsymbol{k}+\boldsymbol{Q}_2}$ cross, e.g., at the X point of the original Brillouin zone (Fig. 12). At half filling and for $mU = 0$ the Fermi level crosses the bands at the X point too; thus the system is insulator for any finite value of mU. In the small-t/U limit we can assume that $m = 1/2$ and expand the eigenvalues in powers of $\varepsilon_{\boldsymbol{k}}/U$. For the occupied states we find

$$\varepsilon_{\boldsymbol{k}-} - \mu \sim -\frac{1}{2}U - \frac{\varepsilon_{\boldsymbol{k}}^2}{U} = -\frac{1}{2}U - \frac{4t^2}{U}\left(\frac{\varepsilon_{\boldsymbol{k}}}{2t}\right)^2.$$

The ground-state total energy for the antiferromagnetic supercell is then $2E_{\rm AF}$ with

$$E_{\rm AF} = -\frac{1}{2}U - \frac{4t^2}{U}\frac{1}{N_{\boldsymbol{k}}}\sum_{\boldsymbol{k}}\left(\frac{\varepsilon_{\boldsymbol{k}}}{2t}\right)^2 \sim -\frac{1}{2}U - \frac{4t^2}{U}$$

so that the energy difference per pair of spins between ferro- and antiferro-magnetic state is

$$\Delta E^{\rm HF} = E^{\rm HF}_{\uparrow\uparrow} - E^{\rm HF}_{\uparrow\downarrow} = \frac{2}{n_{\langle ii'\rangle}}\left[E_{\rm F} - E_{\rm AF}\right] \sim \frac{1}{2}\frac{4t^2}{U} \sim \frac{1}{2}\Gamma, \tag{24}$$

which is similar to the result obtained from the Hubbard model in many-body second order perturbation theory, Eq. (12). Despite the similarity with the actual solution, one has to remember that the spectrum of the Hartree-Fock Hamiltonian has very little to do with the spectrum of the Heisenberg model, the model that describes the actual low-energy behavior of the Hubbard Hamiltonian. If we restrict ourselves to the antiferromagnetic solution, the first excited state is at an energy $\propto U$ rather than $\propto \Gamma$; thus, we cannot use a single HF calculation to understand the magnetic excitation spectrum of a given system. It is more meaningful to use HF to compare

the total energy of different states and determine in this way, within HF, the ground state. Even in this case, however, one has to keep in mind that HF suffers from *spin contamination*, i.e., singlet states and $S_z = 0$ triplet states mix [26]. The energy difference per bond $E^{\rm HF}_{\uparrow\uparrow} - E^{\rm HF}_{\uparrow\downarrow}$ in Eq. (24) only resembles the exact result, as one can grasp by comparing it with the actual energy difference between triplet and singlet state in the two-site Heisenberg model

$$\Delta E = E_{S=1} - E_{S=0} = \Gamma,$$

which is a factor of two larger. The actual ratio $\Delta E/\Delta E^{\rm HF}$ might depend on the details of the HF band structures. Thus, overall, Hartree-Fock is not the ideal approach to determine the onset of magnetic phase transitions. Other shortcomings of the Hartree-Fock approximation are in the description of the Mott metal-insulator transition. In Hartree-Fock the metal-insulator transition is intimately related to long-range magnetic order (Slater transition), but in strongly correlated materials the metal-insulator transition can occur in the paramagnetic phase (Mott transition). It is associated with a divergence of the self-energy at low frequencies rather than with the formation of superstructures. This physics, captured by many-body methods such as the dynamical mean-field theory [15], is completely missed by the Hartree-Fock approximation.

2.3.3 The dynamical mean-field theory approach

The modern approach for solving the Hubbard model is the so-called dynamical mean-field theory method [14–16]. In DMFT the lattice Hubbard model is mapped onto a self-consistent quantum impurity model describing an impurity coupled to a non-correlated conduction-electron bath. The quantum impurity model is typically the Anderson model, which will be discussed in detail in the next chapter. Here we do not want to focus on the specific form of the quantum impurity model but rather on the core aspects of the DMFT approach and on the comparison of DMFT with Hartree-Fock. In Hartree-Fock the effective mean field is an energy-independent (static) parameter; in the example discussed in the previous section it is a function of the magnetic order parameter m. In DMFT the role of the effective mean-field is played by the bath Green function $G_0(i\nu_n)$ where ν_n is a fermionic Matsubara frequency; it is frequency dependent (dynamical) and related to the impurity Green function $G(i\nu_n)$ via the Dyson equation

$$[G(i\nu_n)]^{-1} = [G_0(i\nu_n)]^{-1} - \Sigma(i\nu_n)\,, \tag{25}$$

where $\Sigma(i\nu_n)$ is the impurity self-energy. As in any mean-field theory, the effective field is determined by enforcing a self-consistency condition. In DMFT the latter requires that the impurity Green function $G(i\nu_n)$, calculated by solving the quantum impurity model, equals $G_{ii}(i\nu_n)$, the lattice Green function at a site i

$$G_{ii}(i\nu_n) = G(i\nu_n),$$

with

$$G_{ii}(i\nu_n) = \frac{1}{N_{\boldsymbol{k}}}\sum_{\boldsymbol{k}} G(\boldsymbol{k}; i\nu_n) = \frac{1}{N_{\boldsymbol{k}}}\sum_{\boldsymbol{k}} \frac{1}{i\nu_n - \varepsilon_{\boldsymbol{k}} - \Sigma(i\nu_n) + \mu}.$$

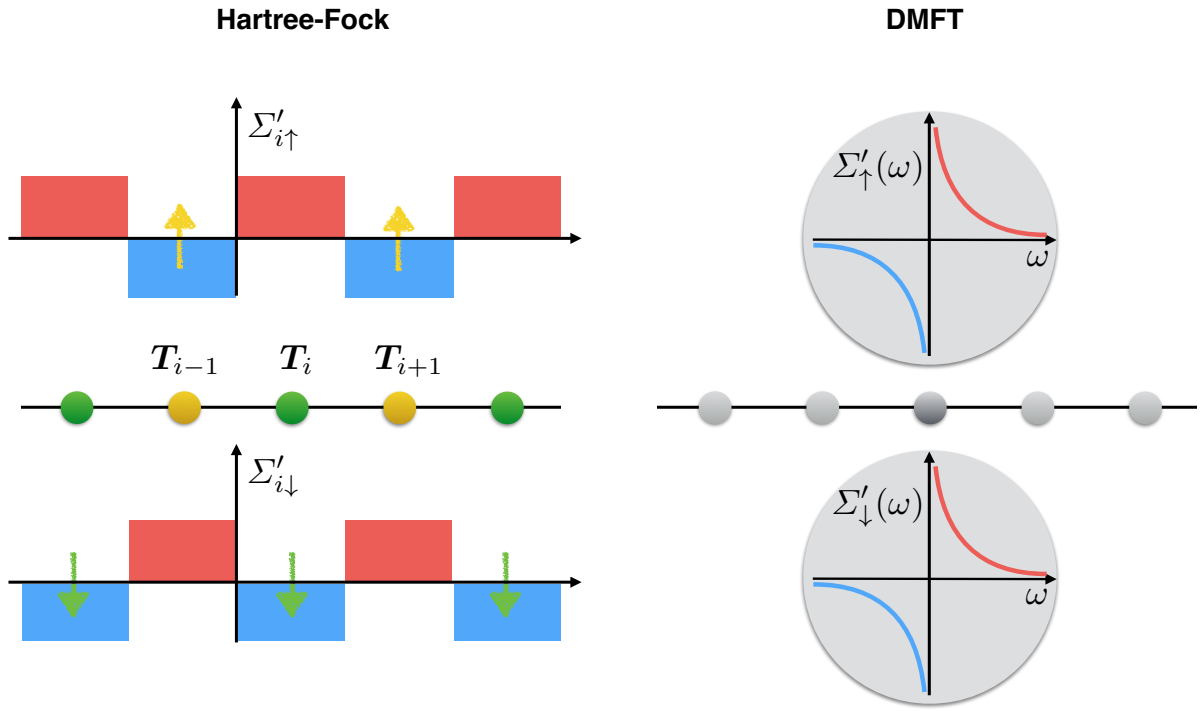

Fig. 13: *Idealized correlated crystal, schematically represented by a half-filled single-band Hubbard chain. Sketch of the real-part of the self-energy in the insulating phase, as described by Hartree-Fock (left-hand side) and DMFT (right-hand side). In HF the self-energy is a spin- and site-dependent potential (Slater insulator). In DMFT it is spin and site independent; it is, however, dynamical and its real part diverges at zero frequency (Mott insulator). The imaginary part of the self-energy is always zero in Hartree-Fock (i.e., quasiparticles have infinite lifetimes).*

The Green function on the real axis can be obtained from $G(i\nu_n)$ via analytic continuation; in the non-interacting case, this can be done simply by replacing $i\nu_n$ with $\omega + i0^+$. The self-energy in Eq. (25) is frequency dependent but local (i.e., site- or $\boldsymbol{k}$-independent); the locality of the self-energy is, of course, an approximation; it becomes an exact property, however, in the limit of infinite coordination number. DMFT yields the exact result in two opposite limits, $t = 0$ (atomic limit) and $U = 0$ (band limit). The first success of DMFT was the description of the paramagnetic Mott metal-insulator transition in the half-filled one-band Hubbard model. It is interesting to examine in more detail the nature of the Mott transition in DMFT and compare it to the Slater transition described by Hartree-Fock. Let us start with analyzing DMFT results. The poles of the Green function, i.e., the solutions of

$$\omega - \varepsilon_{\boldsymbol{k}} - \Sigma'(\omega) = 0\,,$$

where $\Sigma'(\omega)$ is the real part of the self-energy, yield the excitations of our system. In the Fermi liquid regime, the Green function has a pole at zero frequency. Around it, the self-energy has, on the real axis, the following form

$$\Sigma(\omega) \sim \frac{1}{2}\,U + \left(1 - \frac{1}{Z}\right)\omega - \frac{i}{Z\tau^{\mathrm{QP}}}\,,$$

where the positive dimensionless number Z yields the mass enhancement, $m^*/m \sim 1/Z$, and the positive parameter $\tau^{\rm QP} \sim 1/(aT^2 + b\omega^2)$ is the quasiparticles lifetime; at higher frequency the self-energy yields two additional poles corresponding to the Hubbard bands. In the Mott insulating regime the central quasiparticle peak disappears, and only the Hubbard bands remain. The self-energy has approximately the form

$$\Sigma(\omega) \sim \frac{rU^2}{4}\left[\frac{1}{\omega} - i\pi\delta(\omega) - if_U(\omega)\right],$$

where $f_U(\omega)$ is a positive function that is zero inside the gap and r is a model-specific renormalization factor. Hence, the real-part of the self-energy diverges at zero frequency, and there are no well defined low-energy quasiparticles. Furthermore, since we are assuming that the system is paramagnetic, the self-energy and the Green function are independent of the spin

$$\begin{aligned}\Sigma_\sigma(\omega) &= \Sigma(\omega)\\ G_\sigma(\omega) &= G(\omega)\\ G_\sigma(\boldsymbol{k};\omega) &= G(\boldsymbol{k};\omega).\end{aligned}$$

Thus DMFT can be seen, to *some* extent, as a complementary approximation to Hartree-Fock. If we write the Hartree-Fock correction to the energies in the form of a self-energy, the latter is a real, static but spin- and site-dependent potential. More specifically, we have at site i

$$\Sigma^{\rm HF}_{i\sigma}(\omega) = U\left[n^i_{-\sigma} - \frac{1}{2}\right],$$

where n^i_σ is the site occupation for spin σ. Let us consider the antiferromagnetic case. For this, as we have seen, we have to consider two sublattices or a two-site cluster; the magnetization at sites j, nearest neighbors of site i, has opposite sign than at site i. Thus

$$\Sigma^{\rm HF}_{j\sigma}(\omega) = -U\left[n^i_{-\sigma} - \frac{1}{2}\right].$$

This spatial structure of the self-energy is what opens the gap shown in Fig. 12; this picture of the gap opening is very different from the one emerging from DMFT; as we have just seen, in DMFT the gap opens via the divergence at zero frequency in the real-part of the self-energy; this happens already in a single-site paramagnetic calculation, i.e., we do not have to assume any long-range magnetic order. In HF the self-energy resulting from a non-magnetic ($m = 0$) single-site calculation is instead a mere energy shift – the same for all sites and spins – and does not change the band structure at all. Hartree-Fock is not, e.g., the large-U limit of DMFT but merely the large frequency limit of DMFT (or of its cluster extensions). The differences among the two approaches are pictorially shown in Fig. 13 for an idealized one-dimensional crystal.

Let us now focus on the magnetic properties of the Hubbard model, and in particular on the magnetic susceptibility $\chi_{zz}(\boldsymbol{q}; i\omega_m)$. Since in DMFT we solve the quantum impurity model exactly, we can directly calculate the local linear-response tensor, and therefore the local susceptibility $\chi_{zz}(i\omega_m)$. If we are interested in magnetic order, however, we need also, at least

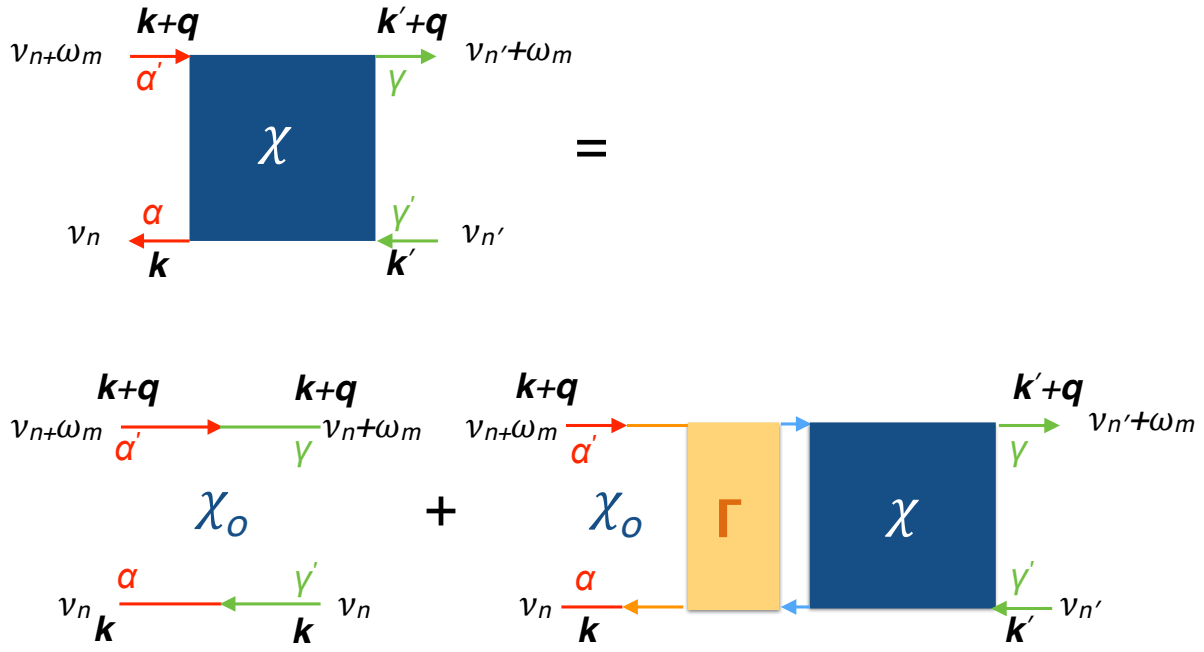

Fig. 14: *Diagrammatic representation of the Bethe-Salpeter equation. In the case of the magnetic susceptibility,* $\alpha = \alpha' = \sigma$ *and* $\gamma = \gamma' = \sigma'$.

in an approximate form, the full $\boldsymbol{q}$-dependent linear-response function, $\chi_{zz}(\boldsymbol{q}; i\omega_m)$. How can we obtain it? It is tempting to think that $\chi_{zz}(\boldsymbol{q}; i\omega_m)$ can be approximated by the bare DMFT susceptibility, $\chi^0_{zz}(\boldsymbol{q}; i\omega_m)$. In the paramagnetic regime, for the one-band Hubbard model this is given by (see Appendix)

$$\chi^0_{zz}(\boldsymbol{q}; i\omega_m) = -\frac{(g\mu_B)^2}{4} \frac{1}{\beta N_{\boldsymbol{k}}} \sum_{\sigma \boldsymbol{k} n} G_\sigma(\boldsymbol{k}; i\nu_n) G_\sigma(\boldsymbol{k}+\boldsymbol{q}; i\nu_n + i\omega_m), \tag{26}$$

where ω_m is a bosonic Matsubara frequency and $G_\sigma(\boldsymbol{k}; i\nu_n)$ is the single-particle Green function for spin σ. Since $\chi^0_{zz}(\boldsymbol{q}; i\omega_m)$ depends only on the single-particle Green function it can be extracted from DMFT calculations with little additional effort. To approximate the actual susceptibility with $\chi^0_{zz}(\boldsymbol{q}; i\omega_m)$ would be, however, totally incorrect. Indeed, while $\chi^0_{zz}(\boldsymbol{q}; i\omega_m)$ is exact in the non-interacting limit (i.e., it correctly yields the Pauli susceptibility for $U = 0$), it is incorrect in the atomic limit ($t = 0$) and hence in the whole local-moment regime. Let us see what happens in the atomic limit. By summing Eq. (26) over $\boldsymbol{q}$, we obtain the local $\chi^0_{zz}(i\omega_m)$, proportional to the sum of products of local Green functions,

$$\chi^0_{zz}(i\omega_m) = -\frac{(g\mu_B)^2}{4} \frac{1}{\beta} \sum_{n\sigma} G_\sigma(i\nu_n) G_\sigma(i\nu_n + i\omega_m).$$

If we replace the local Green functions with the corresponding atomic Green functions (see Appendix) and then perform the Matsubara sums we find the expression

$$\chi^0_{zz}(0) = \frac{(g\mu_B)^2}{4} \frac{\beta e^{\beta U/2}}{1+e^{\beta U/2}} \left[\frac{1}{1+e^{\beta U/2}} + \frac{1}{U\beta} \frac{1-e^{-\beta U}}{1+e^{-\beta U/2}} \right] \underset{\beta U \to \infty}{\sim} \frac{(g\mu_B S)^2}{U},$$

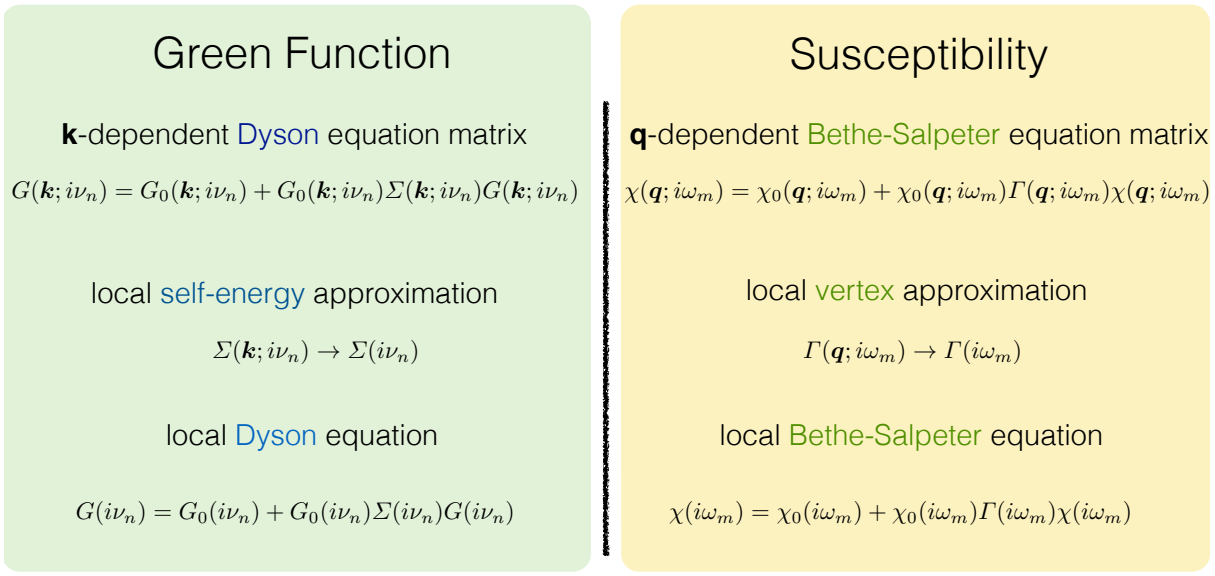

Fig. 15: *Analogies between the Green function $G(\boldsymbol{k};i\nu_n)$ in the local-self-energy approximation (left) and the response function $\chi(\boldsymbol{q};i\omega_m)$ in the local vertex approximation (right). Each term in the Bethe-Salpeter equation is a square matrix of dimension $L_\alpha = N_\alpha N_{\boldsymbol{k}} N_n$, where $N_{\boldsymbol{k}}$ is the number of $\boldsymbol{k}$ points, N_n the number of fermionic Matsubara frequencies, N_α the number of flavors (here: the spin degrees of freedom). The elements of, e.g., the matrix $\chi(\boldsymbol{q};i\omega_m)$ can be written as $[\chi(\boldsymbol{q};i\omega_m)]_{\sigma\boldsymbol{k}\nu_n,\sigma'\boldsymbol{k}'\nu_{n'}}$.*

where the exact result is

$$\chi_{zz}(0) = \frac{1}{4}(g\mu_B)^2 \frac{\beta e^{\beta U/2}}{1+e^{\beta U/2}} \underset{\beta U\to\infty}{\sim} \frac{(g\mu_B S)^2}{k_B T}.$$

Since $\chi^0_{zz}(0)$ is incorrect in the large βU limit, it also does not interpolate properly between the two regimes, weak and strong coupling. Let us then take a step back. The local susceptibility $\chi_{zz}(i\omega_m)$ can be obtained, as we have already mentioned, by solving exactly the self-consistent quantum impurity model, e.g., via quantum Monte Carlo. In a similar way, the $\boldsymbol{q}$-dependent response function $\chi_{zz}(\boldsymbol{q};\omega)$ could in principle be calculated from the solution of the full lattice Hubbard model; the problem is that, unfortunately, the exact solution of the Hubbard model is not available in the general case. If many-body perturbation theory converges, however, we can calculate $\chi_{zz}(\boldsymbol{q};\omega)$ by solving the Bethe-Salpeter equation – the analogon of the Dyson equation for the Green function – with $\chi^0_{zz}(\boldsymbol{q};i\omega_n)$ as bare susceptibility. The Bethe-Salpeter equation is represented diagrammatically in Fig. 14. By summing up all diagrams in the series we find

$$[\chi(\boldsymbol{q};i\omega_n)]^{-1} = [\chi_0(\boldsymbol{q};i\omega_n)]^{-1} - \Gamma(\boldsymbol{q};i\omega_n). \tag{27}$$

Here each term is a square matrix with dimension $L_\alpha = N_\alpha N_{\boldsymbol{k}} N_n$, where N_α is the number of flavors (here, the spin degrees of freedom), $N_{\boldsymbol{k}}$ is the number of $\boldsymbol{k}$ points and N_n the number of fermionic Matsubara frequencies. The quantity $\Gamma(\boldsymbol{q};i\omega_n)$ is the vertex function and hides all diagrams appearing in the many-body perturbation series. Finding the exact $\Gamma(\boldsymbol{q};i\omega_n)$ is of

course as difficult as solving the full many-body problem; we therefore have to find a reasonable approximation. In the spirit of DMFT, let us assume that the vertex entering the Bethe-Salpeter equation can be replaced by a local function

$$\Gamma(\boldsymbol{q}; i\omega_n) \to \Gamma(i\omega_n).$$

Furthermore, let us assume that the local vertex solves, in turn, a local version of the Bethe-Salpeter equation

$$\Gamma(i\omega_m) = [\chi_0(i\omega_m)]^{-1} - [\chi(i\omega_m)]^{-1}. \tag{28}$$

The local vertex $\Gamma(i\omega_m)$, calculated via Eq. (28), can then be used to compute the susceptibility from the $\boldsymbol{q}$-dependent Bethe-Salpeter equation Eq. (27). The analogy between the calculation of the susceptibility in the local vertex approximation and that of the Green function in the local self-energy approximation is shown in Fig. 15.

Let us now qualitatively discuss the magnetic susceptibility of the one-band Hubbard model in the Mott-insulating limit. For simplicity, let us now assume that the vertex is static and thus that we can replace all susceptibility matrices in the Bethe-Salpeter equation with the physical susceptibilities, which we obtain by summing over the fermionic Matsubara frequencies and the momenta. For the magnetic susceptibility this means

$$\begin{aligned}\chi_{zz}(\boldsymbol{q}; i\omega_m) =& (g\mu_B)^2 \frac{1}{\beta^2}\frac{1}{4}\sum_{\sigma\sigma'}\sigma\sigma'\sum_{nn'}\frac{1}{N_{\boldsymbol{k}}^2}\sum_{\boldsymbol{k}\boldsymbol{k}'}\frac{1}{\beta}\left[\chi(\boldsymbol{q}; i\omega_m)\right]_{\sigma\boldsymbol{k}\nu_n,\sigma'\boldsymbol{k}'\nu_{n'}} \\ =& (g\mu_B)^2 \int d\tau\; e^{i\omega_m\tau}\;\langle S_z(\tau)S_z(0)\rangle.\end{aligned}$$

In the high-temperature and large-U limit ($\beta U \to \infty$ and $T \gg T_N$) the static local susceptibility is approximatively given by the static atomic susceptibility

$$\chi_{zz}(0) \sim \frac{\mu_{\text{eff}}^2}{k_B T},$$

where $\mu_{\text{eff}}^2 = (g\mu_B)^2 S(S+1)/3$. Therefore the vertex is roughly given by

$$\Gamma(0) \sim \frac{1}{\chi_{zz}^0(0)} - \frac{k_B T}{\mu_{\text{eff}}^2}.$$

The susceptibility calculated with such a local vertex is

$$\chi_{zz}(\boldsymbol{q}; 0) \sim \frac{\mu_{\text{eff}}^2}{k_B T - \mu_{\text{eff}}^2 J(\boldsymbol{q})} \equiv \frac{\mu_{\text{eff}}^2}{k_B(T - T_{\boldsymbol{q}})},$$

where the coupling is given by

$$J(\boldsymbol{q}) = -\left[\frac{1}{\chi_{zz}^0(\boldsymbol{q}; 0)} - \frac{1}{\chi_{zz}^0(0)}\right].$$

Thus, in the strong-correlation limit, the Bethe-Salpeter equation, solved assuming the vertex is local and, in addition, static, yields a static high-temperature susceptibility of Curie-Weiss form. We had found the same form of the susceptibility by solving the Heisenberg model in the static mean-field approximation. A more detailed presentation of the DMFT approach to calculate linear-response functions can be found in Ref. [27].

3 The Anderson model

The Kondo impurity is a representative case of a system that exhibits both local-moment and Pauli-paramagnetic behavior, although in quite different temperature regimes [12]. The Kondo effect was first observed in diluted metallic alloys, metallic systems in which isolated d or f magnetic impurities are present, and it has been a riddle for decades. A Kondo impurity in a metallic host can be described by the Anderson model

$$H_{\rm A} = \underbrace{\sum_{\sigma}\sum_{\boldsymbol{k}} \varepsilon_{\boldsymbol{k}} n_{\boldsymbol{k}\sigma} + \sum_{\sigma} \varepsilon_f n_{f\sigma} + U n_{f\uparrow} n_{f\downarrow}}_{H_0} + \underbrace{\sum_{\sigma}\sum_{\boldsymbol{k}} \left[V_{\boldsymbol{k}} c^\dagger_{\boldsymbol{k}\sigma} c_{f\sigma} + h.c. \right]}_{H_1}, \tag{29}$$

where ε_f is the impurity level (occupied by $n_f \sim 1$ electrons), $\varepsilon_{\boldsymbol{k}}$ is the dispersion of the metallic band, and $V_{\boldsymbol{k}}$ the hybridization. If we assume that the system has particle-hole symmetry with respect to the Fermi level, then $\varepsilon_f - \mu = -U/2$. The Kondo regime is characterized by the parameter values $\varepsilon_f \ll \mu$ and $\varepsilon_f + U \gg \mu$ and by a weak hybridization, i.e., the hybridization width

$$\Delta(\varepsilon) = \pi \frac{1}{N_{\boldsymbol{k}}} \sum_{\boldsymbol{k}} |V_{\boldsymbol{k}}|^2 \delta(\varepsilon_{\boldsymbol{k}} - \varepsilon)$$

is such that $\Delta(\mu) \ll |\mu - \varepsilon_f|, |\mu - \varepsilon_f - U|$. The Anderson model is also used as the quantum impurity problem in dynamical mean-field theory. In DMFT the bath parameters $\varepsilon_{\boldsymbol{k}}$ and $V_{\boldsymbol{k}}$ have, in principle, to be determined self-consistently. If quantum Monte Carlo is used to solve the Anderson model, it is sufficient to determine the bath Green function self-consistently.

3.1 The Kondo limit

Through the Schrieffer-Wolff canonical transformation [28] one can map the Anderson model onto the Kondo model, in which only the effective spin of the impurity enters

$$H_{\rm K} = H_0' + \Gamma \boldsymbol{S}_f \cdot \boldsymbol{s}_c(\boldsymbol{0}) = H_0' + H_\Gamma, \tag{30}$$

where

$$\Gamma \sim -2|V_{k_F}|^2 \left[\frac{1}{\varepsilon_f} - \frac{1}{\varepsilon_f + U} \right] > 0$$

is the antiferromagnetic coupling arising from the hybridization, $\boldsymbol{S}_f$ the spin of the impurity ($S_f = 1/2$), and $\boldsymbol{s}_c(\boldsymbol{0})$ is the spin-density of the conduction band at the impurity site. For convenience we set the Fermi energy to zero; k_F is a $\boldsymbol{k}$ vector at the Fermi level. The Schrieffer-Wolff canonical transformation works as follows. We introduce the operator S that transforms the Hamiltonian H into H_S

$$H_S = e^S H e^{-S}.$$

We search for an operator S such that the transformed Hamiltonian H_S has no terms of first order in $V_{\boldsymbol{k}}$. Let us first split the original Hamiltonian H_A into two pieces: H_0, the sum of all terms except the hybridization term, and H_1, the hybridization term. Let us choose S linear in $V_{\boldsymbol{k}}$ and such that

$$[S, H_0] = -H_1. \tag{31}$$

From Eq. (31) one finds that the operator S is given by

$$S = \sum_{\boldsymbol{k}\sigma} \left[\frac{1 - n_{f-\sigma}}{\varepsilon_{\boldsymbol{k}} - \varepsilon_f} + \frac{n_{f-\sigma}}{\varepsilon_{\boldsymbol{k}} - \varepsilon_f - U} \right] V_{\boldsymbol{k}} c^\dagger_{\boldsymbol{k}\sigma} c_{f\sigma} - \text{h.c.}.$$

The transformed Hamiltonian is complicated, as can be seen from explicitly writing the series for a transformation satisfying Eq. (31)

$$H_S = H_0 + \frac{1}{2}[S, H_1] + \frac{1}{3}\Big[S, [S, H_1]\Big] + \ldots.$$

In the limit in which the hybridization strength Γ is small this series can, however, be truncated at second order. The resulting Hamiltonian has the form $H_S = H_0 + H_2$, with $H_2 = H_\Gamma + H_{\rm dir} + \Delta H_0 + H_{\rm ch}$. The first term is the exchange interaction

$$H_\Gamma = \frac{1}{4} \sum_{\boldsymbol{k}\boldsymbol{k}'} \Gamma_{\boldsymbol{k}\boldsymbol{k}'} \left[\sum_{\sigma_1\sigma_2} c^\dagger_{\boldsymbol{k}'\sigma_1} \langle \sigma_1 | \hat{\sigma} | \sigma_2 \rangle c_{\boldsymbol{k}\sigma_2} \cdot \sum_{\sigma_3\sigma_4} c^\dagger_{f\sigma_3} \langle \sigma_3 | \hat{\sigma} | \sigma_4 \rangle c_{f\sigma_4} \right]$$

where

$$\Gamma_{\boldsymbol{k}\boldsymbol{k}'} = V^*_{\boldsymbol{k}} V_{\boldsymbol{k}'} \left[\frac{1}{\varepsilon_{\boldsymbol{k}} - \varepsilon_f} + \frac{1}{\varepsilon_{\boldsymbol{k}'} - \varepsilon_f} + \frac{1}{U + \varepsilon_f - \varepsilon_{\boldsymbol{k}}} + \frac{1}{U + \varepsilon_f - \varepsilon_{\boldsymbol{k}'}} \right].$$

Let us assume that the coupling $\Gamma_{\boldsymbol{k}\boldsymbol{k}'}$ is weakly dependent on $\boldsymbol{k}$ and $\boldsymbol{k}'$; then by setting $|\boldsymbol{k}| \sim k_F$, and $|\boldsymbol{k}'| \sim k_F$ we recover the antiferromagnetic contact coupling in Eq. (30).
The second term is a potential-scattering interaction

$$H_{\rm dir} = \sum_{\boldsymbol{k}\boldsymbol{k}'} \left[A_{\boldsymbol{k}\boldsymbol{k}'} - \frac{1}{4}\Gamma_{\boldsymbol{k}\boldsymbol{k}'} \hat{n}_f \right] \sum_\sigma \hat{c}^\dagger_{\boldsymbol{k}'\sigma} \hat{c}_{\boldsymbol{k}\sigma},$$

where

$$A_{\boldsymbol{k}\boldsymbol{k}'} = \frac{1}{2} V^*_{\boldsymbol{k}} V_{\boldsymbol{k}'} \left[\frac{1}{\varepsilon_{\boldsymbol{k}} - \varepsilon_f} + \frac{1}{\varepsilon_{\boldsymbol{k}'} - \varepsilon_f} \right].$$

This term is spin-independent, and thus does not play a relevant role in the Kondo effect. The next term merely modifies the H_0 term

$$\Delta H_0 = -\sum_{\boldsymbol{k}\sigma} \left[A_{\boldsymbol{k}\boldsymbol{k}} - \frac{1}{2}\Gamma_{\boldsymbol{k}\boldsymbol{k}}\, \hat{n}_{f-\sigma} \right] \hat{n}_{f\sigma}.$$

Finally, the last term is a pair-hopping interaction, which changes the charge of the f sites by two electrons and thus can be neglected if $n_f \sim 1$

$$\Delta H_{\rm ch} = -\frac{1}{4}\sum_{\boldsymbol{k}\boldsymbol{k}'\sigma} \Gamma_{\boldsymbol{k}\boldsymbol{k}'} c^\dagger_{\boldsymbol{k}'-\sigma} c^\dagger_{\boldsymbol{k}\sigma} c_{f\sigma} c_{f-\sigma} + \text{h.c.}.$$

The essential term in H_2 is the exchange term H_Γ, which is the one that yields the antiferromagnetic contact interaction in the Kondo Hamiltonian (30). Remarkably, the Schrieffer-Wolff transformation generates a perturbation series in the hybridization; an analogous perturbation series is also used in the hybridization-expansion continuous-time quantum Monte Carlo approach to solve the quantum impurity problem in dynamical mean-field theory.

3.1.1 The impurity susceptibility

The solution of the problem defined by (29) or (30) is not at all trivial and requires many-body techniques such as the Wilson numerical renormalization group [30] or the Bethe ansatz [31]. Here we only discuss some important exact results concerning the magnetic properties. Let us define the *impurity susceptibility* $\chi^f_{zz}(T)$ as the total susceptibility minus the contribution of the metallic band in the absence of the impurity [30–32]. One can show that at high temperatures $\chi^f_{zz}(T)$ has the following behavior

$$\chi^f_{zz}(T) \sim \frac{(g\mu_B)^2 S_f(S_f+1)}{3k_B T}\left\{1 - \frac{1}{\ln\left(T/T_{\rm K}\right)}\right\}.$$

This expression resembles the Curie susceptibility, apart from the $\ln(T/T_{\rm K})$ term. The scale $T_{\rm K}$ is the Kondo temperature, which, to first approximation, is given by

$$k_B T_{\rm K} \sim D e^{-2/\rho(\varepsilon_F)\Gamma},$$

where $2D = W$ is the band width of the host conduction band. Because of the $\ln\left(T/T_{\rm K}\right)$ term, the susceptibility apparently diverges at $T \sim T_{\rm K}$. In reality, however, around $T_{\rm K}$ there is a crossover to a new regime. For $T \ll T_{\rm K}$

$$\chi^f_{zz}(T) \sim \frac{C_{1/2}}{\mathcal{W} T_{\rm K}}\left\{1 - \alpha T^2 + \dots\right\},$$

where $\mathcal{W}$ is a (universal) Wilson number. Thus the low-temperature system has a Fermi liquid behavior with enhanced density of states, i.e., with heavy masses m^*/m; furthermore $\chi^f_{zz}(0) = C_{1/2}/\mathcal{W}T_{\rm K}$ is the Curie susceptibility (Eq. (15)) with the temperature *frozen* at $T = \mathcal{W}T_{\rm K}$. At $T = 0$ the impurity magnetic moment is screened by the conduction electrons, which form a singlet state with the spin of the impurity. In other words, the effective magnetic moment formed by the impurity magnetic moment and its screening cloud,

$$\mu^2_{\rm eff}(T) \equiv 3k_B T \chi^f_{zz}(T) \propto \langle S^f_z S^f_z\rangle + \langle S^f_z s^c_z\rangle,$$

vanishes for $T \ll T_{\rm K}$. The Kondo temperature is typically 10–30 K or even smaller, hence the Fermi liquid behavior is restricted to a very narrow energy and temperature region.

3.1.2 Poor man's scaling

We can understand the existence of a Fermi liquid regime by using a simple approach due to Anderson called *poor man's scaling* [33] and an argument due to Nozières. First we divide the Hilbert space into a high- and a low-energy sector. We define as *high-energy* states those with at least one electron or one hole at the top or bottom of the band; the corresponding constraint for the high-energy electronic level $\varepsilon_{\boldsymbol{q}}$ is $D' < \varepsilon_{\boldsymbol{q}} < D$ or $-D < \varepsilon_{\boldsymbol{q}} < -D'$, where $D' = D - \delta D$. Next we introduce the operator P_H, which projects onto the high-energy states, and the operator $P_L = 1 - P_H$, which projects onto states with no electrons or holes in the high-energy region. Then we downfold the high-energy sector of the Hilbert space. To do this we rewrite the original Kondo Hamiltonian, $H \equiv H_0' + H_\Gamma$, as the energy-dependent operator H', which acts only in the low-energy sector

$$\begin{aligned} H' &= P_L H P_L + \delta H_L = H_L + \delta H_L, \\ \delta H_L &= P_L H P_H \left(\omega - P_H H P_H\right)^{-1} P_H H P_L. \end{aligned}$$

Here H_L is the original Hamiltonian, however in the space in which the high-energy states have been eliminated; the term δH_L is a correction due to the interaction between low and (downfolded) high-energy states. Up to this point, the operator H' has the same spectrum of the original Hamiltonian. To make use of this expression, however, we have to introduce approximations. Thus, let us calculate δH_L using many-body perturbation theory. The first non-zero contribution is of second order in Γ

$$\delta H_L^{(2)} \sim P_L H_\Gamma P_H \left(\omega - P_H H_0' P_H\right)^{-1} P_H H_\Gamma P_L \,.$$

There are two types of processes that contribute at the second order, an electron and a hole process, depending on whether the downfolded states have (at least) one electron or one hole in the high-energy region. Let us consider the electron process. We set

$$P_H \sim \sum_{\boldsymbol{q}\sigma} c_{\boldsymbol{q}\sigma}^\dagger |FS\rangle\langle FS| c_{\boldsymbol{q}\sigma}, \quad P_L \sim \sum_{\boldsymbol{k}\sigma} c_{\boldsymbol{k}\sigma}^\dagger |FS\rangle\langle FS| c_{\boldsymbol{k}\sigma} \,,$$

where $|\varepsilon_{\boldsymbol{k}}| < D'$ and $|FS\rangle = \prod_{\boldsymbol{k}\sigma} c_{\boldsymbol{k}\sigma}^\dagger |0\rangle$ is the Fermi sea, i.e., the many-body state corresponding to the metallic conduction band. Thus

$$\delta H_L^{(2)} = -\frac{1}{2}\Gamma^2 \sum_{\boldsymbol{q}} \frac{1}{\omega - \varepsilon_{\boldsymbol{q}}} \boldsymbol{S}_f \cdot \boldsymbol{s}_c(\boldsymbol{0}) + \ldots \;\sim\; \frac{1}{4}\rho(\varepsilon_F)\Gamma^2 \,\frac{\delta D}{D} \boldsymbol{S}_f \cdot \boldsymbol{s}_c(\boldsymbol{0}) + \ldots .$$

We find an analogous contribution from the hole process. The correction $\delta H_L^{(2)}$ modifies the parameter Γ of the Kondo Hamiltonian as follows

$$\begin{aligned} \Gamma \to \Gamma' &= \Gamma + \delta\Gamma, \\ \frac{\delta\Gamma}{\delta \ln D} &= \frac{1}{2}\rho(\varepsilon_F)\Gamma^2, \end{aligned} \tag{32}$$

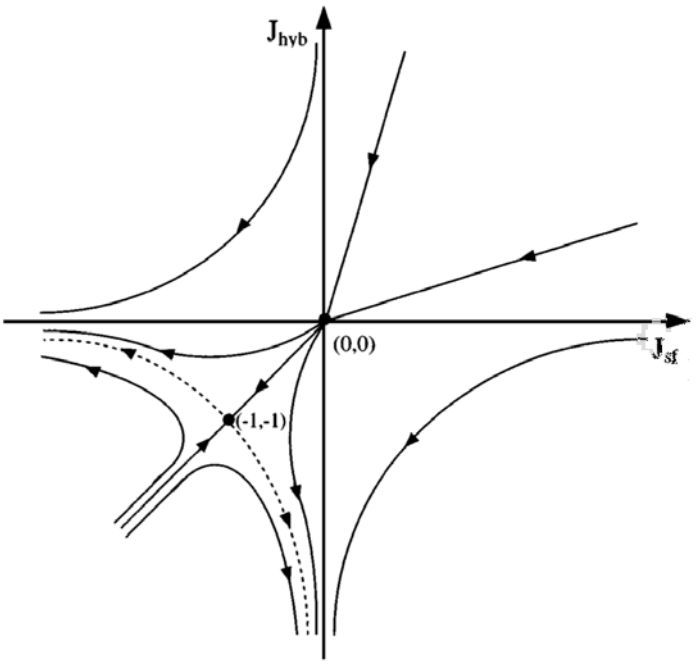

Fig. 16: *Sketch of the scaling diagrams for the two-channel Kondo model.* $\Gamma = -J_{\rm hyb}$ *and* $\Gamma_F = -J_{\rm sf}$. *For* $\Gamma > 0$ *(antiferromagnetic) and* $\Gamma_F < 0$ *(ferromagnetic), the antiferromagnetic coupling scales to strong coupling and ferromagnetic one to weak coupling (right bottom quadrant). From Ref. [34].*

where $\delta \ln D = \delta D/D$. Equation (32) has two fixed points, $\Gamma = 0$ (*weak coupling*) and $\Gamma \to \infty$ (*strong coupling*). By solving the scaling equations we find

$$\Gamma' = \frac{\Gamma}{1 + \frac{1}{2}\rho(\varepsilon_F)\Gamma \ln \frac{D'}{D}}.$$

If Γ is antiferromagnetic the renormalized coupling constant Γ' diverges for $D' = De^{-2/\Gamma\rho(\varepsilon_F)}$, an energy proportional to the Kondo energy $k_B T_{\rm K}$. This divergence (scaling to strong coupling) indicates that at low energy the interaction between the spins dominates, and therefore the system forms a singlet in which the impurity magnetic moment is screened. The existence of this strong coupling fixed point is confirmed by the numerical renormalization group of Wilson [30]. Nozières [35] has used this conclusion to show that the low-temperature behavior of the system must be of Fermi liquid type. His argument is the following. For infinite coupling Γ' the impurity traps a conduction electron to form a singlet state. For a finite but still very large Γ', any attempt at breaking the singlet will cost a very large energy. Virtual excitations (into the $n_f = 0$ or $n_f = 2$ states and finally the $n_f = 1$ triplet state) are however possible and they yield an effective indirect interaction between the remaining conduction electrons surrounding the impurity. This is similar to the phonon-mediated attractive interaction in metals. The indirect electron-electron coupling is weak and can be calculated in perturbation theory ($1/\Gamma$ expansion). Nozières has shown that, to first approximation, the effective interaction is between electrons of opposite spins lying next to the impurity. It is of order D^4/Γ^3 and repulsive, hence it gives rise to a Fermi liquid behavior with enhanced susceptibility [35].

If $\Gamma = \Gamma_F < 0$ (ferromagnetic coupling, as for example the coupling arising from direct Coulomb exchange) the renormalized coupling constant Γ' goes to zero in the $D' \to 0$ limit (scaling to weak coupling). This means that the local spin becomes *asymptotically free* and yields a Curie-type susceptibility, which diverges for $T \to 0$. For small but finite coupling we can account for the ferromagnetic interaction perturbatively (expansion in orders of Γ_F). In f-electron materials often both ferro and antiferromagnetic exchange couplings are present, the first, Γ_F, arising from the Coulomb exchange, the second, Γ, from the hybridization. There are therefore two possibilities. If both exchange interactions couple the impurity with the same conduction channel, only the total coupling $\Gamma_F + \Gamma$ matters. Thus a $|\Gamma_F| > \Gamma$ suppresses the Kondo effect. If, however, ferromagnetic and antiferromagnetic exchange interaction couple the impurity to different conduction channels, a $|\Gamma_F| > \Gamma$ does not suppress the Kondo effect (Fig. 16) but merely reduces $T_{\rm K}$. In the infinite $|\Gamma_F|$ limit the model describes an undercompensated Kondo effect [34].

3.2 The RKKY interaction

The Kondo Hamiltonian (30) describes a magnetic coupling between a local impurity and a bath of conduction electrons. Thus, in the presence of several Kondo impurities coupled to the same conduction electron bath, an indirect magnetic coupling between the local moments arises. Let us start for simplicity from two Kondo impurities described by the Hamiltonian

$$H_{\rm 2K} = \sum_{\boldsymbol{k}\sigma} \varepsilon_{\boldsymbol{k}} n_{\boldsymbol{k}\sigma} + \sum_{i=1,2} \Gamma \boldsymbol{S}_f^i \cdot \boldsymbol{s}_c(\boldsymbol{0}). \tag{33}$$

Let us calculate the effective magnetic coupling between the impurities by integrating out the degrees of freedom of the conduction electrons; this can be done again via perturbation theory or via a canonical transformation. At second order in Γ, the original Hamiltonian becomes

$$H_{\rm RKKY} = I_{12}(\boldsymbol{R}_{12})\ \boldsymbol{S}_f^1 \cdot \boldsymbol{S}_f^2 \tag{34}$$

where $\boldsymbol{R}_{12} = \boldsymbol{R}_1 - \boldsymbol{R}_2$ and

$$I_{12}(\boldsymbol{R}_{12}) \sim -\,\Gamma^2 \frac{1}{N_{\boldsymbol{k}}} \sum_{\boldsymbol{k}} \frac{1}{N_{\boldsymbol{k}}} \sum_{\boldsymbol{q}} \Theta(\varepsilon_F - \varepsilon_{\boldsymbol{k}}) \Theta(\varepsilon_{\boldsymbol{k}+\boldsymbol{q}} - \varepsilon_F) \frac{\cos \boldsymbol{q} \cdot \boldsymbol{R}_{12}}{\varepsilon_{\boldsymbol{k}+\boldsymbol{q}} - \varepsilon_{\boldsymbol{k}}}.$$

For a free-electron gas one finds

$$I_{12}(R_{12}) \sim -\,\frac{\Gamma^2 q_F^4}{\pi^3} \left[\frac{\sin 2q_F R_{12} - 2q_F R_{12} \cos 2q_F R_{12}}{(2q_F R_{12})^4} \right],$$

where $R_{12} = |\boldsymbol{R}_{12}|$. The coupling $I_{12}(R_{12})$ decays as $\sim 1/R_{12}^3$ with the distance between the two impurities. It oscillates with a behavior similar to Friedel oscillations; the sign of the interaction at a certain distance between the impurities depend on the band filling, and it is negative (ferromagnetic) for $q_F \to 0$. The exchange Hamiltonian $H_{\rm RKKY}$ is known as the Ruderman-Kittel-Kasuya-Yosida (RKKY) interaction and competes with the Kondo effect.

We can understand this competition using the following – well known but naive – argument. For simplicity, we assume $I_{12} > 0$ (antiferromagnetic) as it is often the case. The energy gain obtained forming a singlet (antiferromagnetic state) is $E_S \propto -I_{12} \propto -\Gamma^2$; the Kondo energy gain is instead $E_K \propto -k_B T_K \sim -De^{-2/\rho(\varepsilon_F)\Gamma}$. If the coupling constant Γ is small $|E_S|$ is larger than $|E_K|$. In this case, the antiferromagnetic order is favored over the Kondo effect, which would lead to the screening of local moments. In the opposite limit, i.e., when Γ is large, the Kondo effect dominates, and the local moments are screened – thus the system does not exhibit any long-range order. Although reality is more complex – the two effects occur together – this simple argument gives a picture of the mechanisms at play in a lattice of Kondo impurities. It is important to understand that the RKKY interaction is an indirect coupling arising from the interaction of a *correlated* impurity with a conduction-electron bath; the coupling I_{12} is proportional to Γ^2, and the coupling Γ itself was obtained by integrating out high-energy doubly occupied states on the impurity, in a similar way as we have seen for kinetic exchange. In the $U = 0$ limit the coupling Γ diverges and the full construction breaks down. Finally, in a system in which non-perturbative effects – such as the Kondo effect – play a key role, the second order Hamiltonian $H_{\rm RKKY}$ is in general not even sufficient to describe the actual nature of the magnetic phenomena; to obtain $H_{\rm RKKY}$ we have actually integrated out the very interaction leading to the Kondo effect, and this is clearly incorrect in the general case.

4 Conclusion

In this lecture we introduced some of the fundamental aspects of magnetism in correlated systems. We have seen two distinct regimes, the itinerant and the local-moment regime. In the first regime we can, in most cases, treat correlation effects in perturbation theory. In the world of real materials this is the limit in which density-functional theory (DFT), in the local-density approximation or its simple extensions, works best. If the system is weakly correlated we can calculate the linear-response function in the random-phase approximation and understand magnetism within this approach fairly well.

The opposite regime is the strong-correlation limit, in which many-body effects play a key role. In this limit perturbation theory fails and we have in principle to work with many-body methods. If, however, we are interested only in magnetic phenomena, at integer filling a strong simplification comes from mapping the original many-body Hamiltonian into an effective spin model. The exact solution of effective spin models requires in general numerical methods such as the Monte Carlo or quantum Monte Carlo approach, or, when the system is small enough, exact diagonalization or Lanczos. To work with material-specific spin models we need to calculate the magnetic exchange parameters. Typically this is done starting from total-energy DFT calculations for different spin configurations, e.g., in the LDA+U approximation. The LDA+U approach is based on the Hartree-Fock approximation, and therefore when we extract the parameters from LDA+U calculations we have to keep in mind the shortcomings of the method. Furthermore if we want to extract the magnetic couplings from total energy calculations we have to make a guess on the form of the spin model. More flexible approaches, which allow

us to account for actual correlation effects, are based on Green functions and the local-force theorem [36], or on canonical transformations [28, 37].
In strongly correlated materials localized- and itinerant-moment physics can often be observed in the same system, although in different energy or temperature regimes. This is apparent in the case of the Kondo effect. For a Kondo impurity, the susceptibility exhibits a Curie behavior at high temperature and a Fermi liquid behavior at low temperature. In correlated transition-metal oxides Fermi liquid and local-spin magnetism can both play an important role but at different energy scales. Furthermore, in the absence of a large charge gap, downfolding to spin models is not really justified. The modern method to bridge between the localized and itinerant regimes and deal with the actual complications of real systems is the dynamical mean-field theory (DMFT) [14–16]. Within this technique we directly solve generalized Hubbard-like models, albeit in the local self-energy approximation. DMFT is the first flexible approach that allows us to understand the paramagnetic Mott metal-insulator transition and thus also magnetism in correlated materials in a realistic setting. Modern DMFT codes are slowly but steadily becoming as complex and flexible as DFT codes, allowing us to deal with the full complexity of strongly correlated materials. While this is a huge step forward, we have to remember that state-of-the-art many-body techniques have been developed by solving simple models within certain approximations. We have to know these very well if we want to understand real materials and further advance the field. In DMFT we self-consistently solve an effective quantum impurity model, a generalization of the Anderson model. Thus a lot can be learnt from the solution of the Anderson model in the context of the Kondo problem. Much can be understood alone with simple arguments, as Anderson or Nozières have shown us, reaching important conclusions on the Kondo problem with paper and pencil.

Acknowledgment

Support of the Deutsche Forschungsgemeinschaft through FOR1346 is gratefully acknowledged.

Appendices

A Formalism

The formulas in this Appendix are in atomic units: The numerical value of e, m, and $\hbar$ is 1, that of μ_B is either $1/2$ (SI units) or $\alpha/2$ (cgs-Gauss units), where α is the fine-structure constant; the energies are in Hartree.

A.1 Matsubara Green functions

A.1.1 Imaginary-time and frequency Green functions

The imaginary-time Matsubara Green function is defined as

$$G_{\alpha\alpha'}(\boldsymbol{\tau}) = -\langle \mathcal{T} c_\alpha(\tau_1) c^\dagger_{\alpha'}(\tau_2)\rangle = -\frac{1}{Z}\mathrm{Tr}\ \left[e^{-\beta(H-\mu N)}\mathcal{T} c_\alpha(\tau_1) c^\dagger_{\alpha'}(\tau_2)\right],$$

where $\mathcal{T}$ is the time-ordering operator, $\boldsymbol{\tau} = (\tau_1, \tau_2)$, $Z = \mathrm{Tr} e^{-\beta(H-\mu N)}$ is the partition function, and the imaginary-time operators $o(\tau) = c(\tau), c^\dagger(\tau)$ are defined as

$$o(\tau) = e^{\tau(H-\mu N)} o\ e^{-\tau(H-\mu N)}.$$

The indices α and α' are the flavors; they can be site and spin indices in the atomic limit and $\boldsymbol{k}$ and spin indices in the non-interacting-electrons limit. Writing the action of the time-ordering operator explicitly, we obtain

$$G_{\alpha\alpha'}(\boldsymbol{\tau}) = -\Theta(\tau_1-\tau_2)\langle c_\alpha(\tau_1) c^\dagger_{\alpha'}(\tau_2)\rangle + \Theta(\tau_2-\tau_1)\langle c^\dagger_{\alpha'}(\tau_2) c_\alpha(\tau_1)\rangle.$$

Using the invariance of the trace of the product of operators under cyclic permutations, one can show that the following properties hold

$$\begin{aligned} G_{\alpha\alpha'}(\boldsymbol{\tau}) &= \quad G_{\alpha\alpha'}(\tau_1-\tau_2), \\ G_{\alpha\alpha'}(\tau) &= -G_{\alpha\alpha'}(\tau+\beta) \qquad \text{for } -\beta < \tau < 0. \end{aligned}$$

The Fourier transform on the Matsubara axis is

$$G_{\alpha\alpha'}(i\nu_n) = \frac{1}{2}\int_{-\beta}^{\beta} d\tau e^{i\nu_n\tau} G_{\alpha\alpha'}(\tau) = \int_0^\beta d\tau e^{i\nu_n\tau} G_{\alpha\alpha'}(\tau),$$

with $\nu_n = (2n+1)\pi/\beta$. The inverse Fourier transform is given by

$$G_{\alpha\alpha'}(\tau) = \frac{1}{\beta}\sum_{n=-\infty}^{+\infty} e^{-i\nu_n\tau} G_{\alpha\alpha'}(i\nu_n).$$

The convergence of $G_{\alpha\alpha'}(\tau)$ is only guaranteed in the interval $-\beta < \tau < \beta$. Finally, if n_α is the number of electrons for flavor α, one can show that

$$G_{\alpha\alpha}(\tau \to 0^+) = -1 + n_\alpha, \quad G_{\alpha\alpha}(\tau \to \beta^-) = -n_\alpha. \tag{35}$$

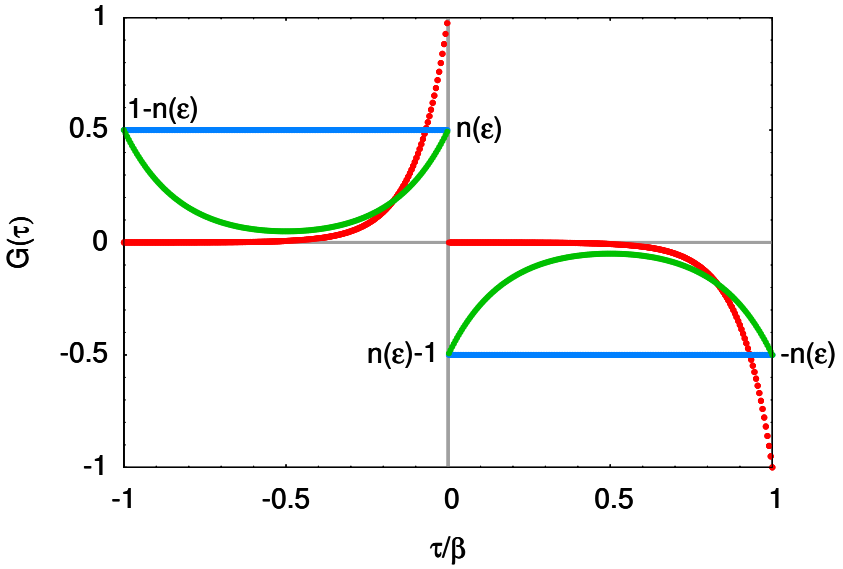

Fig. 17: *The function $\mathcal{G}_{\boldsymbol{k}\sigma}(\tau)$ defined in Eq. (37) for a state well below the Fermi level (red) and at the Fermi level (blue) for $\beta = 2$ (eV)$^{-1}$. The green line shows the atomic $G(\tau)$ from Eq. (39) for $U = 6$ eV and magnetic field $h = 0$.*

A.1.2 Non-interacting limit

For a non-interacting system described by the Hamiltonian

$$H_0 = \sum_{\boldsymbol{k}\sigma} \varepsilon_{\boldsymbol{k}} n_{\boldsymbol{k}\sigma} \tag{36}$$

we can show that the imaginary time Green function $\mathcal{G}_{\boldsymbol{k}\sigma}(\tau)$ is given by

$$\begin{aligned} \mathcal{G}_{\boldsymbol{k}\sigma}(\tau) &= -\left\langle \mathcal{T}\left[c_{\boldsymbol{k}\sigma}(\tau) c^{\dagger}_{\boldsymbol{k}\sigma}(0)\right]\right\rangle \\ &= -\Big[\Theta(\tau)\left(1 - n_\sigma(\varepsilon_{\boldsymbol{k}})\right) - \Theta(-\tau) n_\sigma(\varepsilon_{\boldsymbol{k}})\Big] e^{-(\varepsilon_{\boldsymbol{k}}-\mu)\tau}, \end{aligned} \tag{37}$$

where $n_\sigma(\varepsilon_{\boldsymbol{k}})$ is the occupation number

$$n_\sigma(\varepsilon_{\boldsymbol{k}}) = \frac{1}{1 + e^{\beta(\varepsilon_{\boldsymbol{k}}-\mu)}}.$$

The Fourier transform of the Green function $\mathcal{G}_{\boldsymbol{k}\sigma}(\tau)$ at the Matsubara frequencies is

$$\mathcal{G}_{\boldsymbol{k}\sigma}(i\nu_n) = \frac{1}{i\nu_n - (\varepsilon_{\boldsymbol{k}} - \mu)}.$$

To obtain the analytic continuation of this Green function on the real axis we substitute

$$i\nu_n \to \omega + i0^+.$$

A.1.3 Matsubara sums

The non-interacting Green function $\mathcal{G}_{\boldsymbol{k}\sigma}(z)$ has a pole at $z_p = \varepsilon_{\boldsymbol{k}} - \mu$; the Fermi function $n_\sigma(z)$ has poles for $z = i\nu_n$ instead. Let us consider the integral

$$\frac{1}{2\pi i}\oint_C \mathcal{F}_{\boldsymbol{k}\sigma}(z) n_\sigma(z) e^{z\tau} dz = 0,$$

where $0 < \tau < \beta$ and where the function $\mathcal{F}_{\boldsymbol{k}\sigma}(z)$ is analytic everywhere except at some poles $\{z_p\}$. The contour C is a circle in the full complex plane centered at the origin and including the poles of the Fermi function (Matsubara frequencies) and the poles of $\mathcal{F}_{\boldsymbol{k}\sigma}(z)$. The integral is zero because the integrand vanishes exponentially for $|z| \to \infty$. Furthermore

$$\text{Res } [n_\sigma(i\nu_n)] = -\frac{1}{\beta}.$$

Using Cauchy's integral theorem we then have

$$\frac{1}{\beta}\sum_n e^{i\nu_n\tau}\mathcal{F}_{\boldsymbol{k}\sigma}(i\nu_n) = \sum_{z_p} \text{Res } [\mathcal{F}_{\boldsymbol{k}\sigma}(z_p)]\, n_\sigma(z_p) e^{z_p\tau}.$$

We can use this expression and (35) to show that

$$\frac{1}{\beta}\sum_n e^{-i\nu_n 0^-}\mathcal{G}_{\boldsymbol{k}\sigma}(i\nu_n) = \mathcal{G}_{\boldsymbol{k}\sigma}(0^-) = n_\sigma(\varepsilon_{\boldsymbol{k}}),$$
$$\frac{1}{\beta}\sum_n e^{-i\nu_n 0^+}\mathcal{G}_{\boldsymbol{k}\sigma}(i\nu_n) = \mathcal{G}_{\boldsymbol{k}\sigma}(0^+) = n_\sigma(\varepsilon_{\boldsymbol{k}}) - 1.$$

In a similar way we can show that

$$\frac{1}{\beta}\sum_n e^{i\nu_n 0^+}\mathcal{G}_{\boldsymbol{k}\sigma}(i\nu_n)\mathcal{G}_{\boldsymbol{k}\sigma}(i\nu_n) = \frac{dn_\sigma(\varepsilon_{\boldsymbol{k}})}{d\varepsilon_{\boldsymbol{k}}} = \beta n_\sigma(\varepsilon_{\boldsymbol{k}})[-1 + n_\sigma(\varepsilon_{\boldsymbol{k}})],$$

$$\frac{1}{\beta}\sum_n e^{i\nu_n 0^+}\mathcal{G}_{\boldsymbol{k}\sigma}(i\nu_n)\mathcal{G}_{\boldsymbol{k}+\boldsymbol{q}\sigma}(i\nu_n + i\omega_m) = \frac{n_{\boldsymbol{k}+\boldsymbol{q}} - n_{\boldsymbol{k}}}{-i\omega_m + \varepsilon_{\boldsymbol{k}+\boldsymbol{q}} - \varepsilon_{\boldsymbol{k}}},$$

where in the last relation $\omega_m = 2m\pi/\beta$ is a bosonic Matsubara frequency.

A.1.4 Atomic limit

It is interesting to consider a half-filled idealized atom described by the Hamiltonian

$$H = \varepsilon_d \sum_\sigma n_\sigma + U\left(\frac{N^2}{4} - S_z^2\right) + g\mu_B h S_z. \tag{38}$$

For $\tau > 0$ we can calculate explicitly the Green function, obtaining

$$G_\sigma(\tau) = -\frac{1}{2}\frac{1}{1 + e^{\beta U/2}\cosh\left(\beta g\mu_B h/2\right)}\left[e^{\tau(U - g\mu_B h\sigma)/2} + e^{(\beta-\tau)(U+g\mu_B h\sigma)/2}\right]. \tag{39}$$

The Fourier transform of $G_\sigma(\tau)$ is

$$G_\sigma(i\nu_n) = \left[\frac{w_-}{i\nu_n + (U - g\mu_B h\sigma)/2} + \frac{w_+}{i\nu_n - (U + g\mu_B h\sigma)/2}\right],$$

where

$$w_\pm = \frac{1}{2}\frac{1 + e^{\beta U/2} e^{\pm\beta g\mu_B h\sigma/2}}{1 + e^{\beta U/2}\cosh(\beta g\mu_B h/2)}.$$

Since the Green function is written as the sum of functions with one pole, the analytic continuation is simple, as in the non-interacting case. We replace $i\nu_n$ with $\omega + i0^+$.

A.2 Linear-response theory

A.2.1 Theory

The response of a system described by the Hamiltonian H to a small magnetic field $\boldsymbol{h}(\boldsymbol{r}, t)$ is given by the linear correction to the Hamiltonian, i.e.,

$$\sum_\nu \delta H_\nu(\boldsymbol{r}; t) = -\sum_\nu M_\nu(\boldsymbol{r}; t) h_\nu(\boldsymbol{r}; t), \tag{40}$$

where $\boldsymbol{M}(\boldsymbol{r}; t)$ is the magnetization operator in the Heisenberg representation

$$M_\nu(\boldsymbol{r}; t) = e^{iHt} M_\nu(\boldsymbol{r}) e^{-iHt}$$

and $\nu = x, y, z$. To linear order in the perturbation and assuming that the perturbation is turned on adiabatically at $t_0 = -\infty$

$$\underbrace{\langle M_\nu(\boldsymbol{r}; t)\rangle - \langle M_\nu(\boldsymbol{r})\rangle_0}_{\delta\langle M_\nu(\boldsymbol{r}; t)\rangle} = -i\sum_{\nu'}\int d\boldsymbol{r}' \int_{-\infty}^{t} dt' \langle[\Delta M_\nu(\boldsymbol{r}; t), \delta H_{\nu'}(\boldsymbol{r}'; t')]\rangle_0.$$

Here $\langle M_\nu(\boldsymbol{r})\rangle_0$ is the (equilibrium) thermal average in the absence of the perturbation and $\Delta M_\nu(\boldsymbol{r}; t) = M_\nu(\boldsymbol{r}; t) - \langle M_\nu(\boldsymbol{r})\rangle_0$. By replacing $\sum_{\nu'} \delta H_{\nu'}(\boldsymbol{r}'; t')$ with (40) we obtain

$$\delta\langle M_\nu(\boldsymbol{r}; t)\rangle = i\sum_{\nu'}\int d\boldsymbol{r}' \int_{-\infty}^{t} dt' \,\langle[\Delta M_\nu(\boldsymbol{r}; t), \Delta M_{\nu'}(\boldsymbol{r}'; t')]\rangle_0 \, h_{\nu'}(\boldsymbol{r}'; t').$$

The function

$$\chi_{\nu\nu'}(\boldsymbol{r}, \boldsymbol{r}'; t, t') = i\,\langle[\Delta M_\nu(\boldsymbol{r}; t), \Delta M_{\nu'}(\boldsymbol{r}'; t')]\rangle_0 \,\Theta(t - t') \tag{41}$$

is the so-called retarded response function. If the Hamiltonian H has time translational invariance symmetry the retarded response function depends only on time differences $t - t'$. For the Fourier transform, we have

$$\delta\langle M_\nu(\boldsymbol{r}; \omega)\rangle = \sum_{\nu'}\int d\boldsymbol{r}' \chi_{\nu\nu'}(\boldsymbol{r}, \boldsymbol{r}'; \omega) h_{\nu'}(\boldsymbol{r}'; \omega).$$

For a system with translational invariance, we additionally have

$$\delta\langle M_\nu(\boldsymbol{q};\omega)\rangle = \sum_{\nu'} \chi_{\nu\nu'}(\boldsymbol{q};\omega) h_{\nu'}(\boldsymbol{q};\omega).$$

In the $\omega = 0$ and $\boldsymbol{q} \to \boldsymbol{0}$ limit we have

$$\chi_{\nu\nu'}(\boldsymbol{0};0) = \lim_{h_{\nu'}\to 0} \frac{\partial M_\nu}{\partial h_{\nu'}},$$

where $h_{\nu'} = h_{\nu'}(\boldsymbol{0};0)$. More details can be found in Ref. [27]. In the rest of the Appendix we replace for simplicity the notation $\langle\cdots\rangle_0$ with $\langle\cdots\rangle$.

A.2.2 Kramers-Kronig relations and thermodynamic sum rule

Important properties of the spin susceptibility are the Kramers-Kronig relations

$$\mathrm{Re}[\chi(\boldsymbol{q};\omega)] - \mathrm{Re}[\chi(\boldsymbol{q};\infty)] = \frac{1}{\pi}\mathcal{P}\int_{-\infty}^{+\infty} \frac{\mathrm{Im}[\chi(\boldsymbol{q};\omega')]}{\omega'-\omega} d\omega',$$

$$\mathrm{Im}[\chi(\boldsymbol{q};\omega)] = -\frac{1}{\pi}\mathcal{P}\int_{-\infty}^{+\infty} \frac{\mathrm{Re}[\chi(\boldsymbol{q};\omega')] - \mathrm{Re}[\chi(\boldsymbol{q};\infty)]}{\omega'-\omega} d\omega',$$

where $\mathcal{P}$ is the Cauchy principal value, and Re and Im indicate the real and imaginary part. The first Kramers-Kronig relation yields the sum rule

$$\mathrm{Re}[\chi(\boldsymbol{q};\omega=0)] - \mathrm{Re}[\chi(\boldsymbol{q};\infty)] = \frac{1}{\pi}\mathcal{P}\int_{-\infty}^{+\infty} \frac{\mathrm{Im}[\chi(\boldsymbol{q};\omega')]}{\omega'} d\omega'. \tag{42}$$

In the $\boldsymbol{q} = \boldsymbol{0}$ limit, Eq. (42) is known as *thermodynamic sum rule*.

A.2.3 Fluctuation-dissipation theorem and static susceptibility

We define the spin-spin correlation function

$$\mathcal{S}_{\nu\nu'}(\boldsymbol{q};t) = \langle\, \Delta S_\nu(\boldsymbol{q};t) \Delta S_{\nu'}(-\boldsymbol{q})\rangle$$

where $\Delta S_\nu(\boldsymbol{q};t) = S_\nu(\boldsymbol{q};t) - \langle S_\nu(\boldsymbol{q};0)\rangle$ and where the S_ν are spin operators. The Fourier transform of the correlation function in frequency space is $\mathcal{S}_{\nu\nu'}(\boldsymbol{q};\omega)$. One can show that

$$\mathcal{S}_{\nu\nu'}(\boldsymbol{q};\omega) = e^{\beta\omega}\mathcal{S}_{\nu'\nu}(\boldsymbol{q};-\omega).$$

The following formula, known as fluctuation-dissipation theorem, relates the spin-spin correlation function with the magnetic susceptibility

$$\mathrm{Im}[\chi_{\nu\nu'}(\boldsymbol{q};\omega)] = \frac{1}{2(1+n_B)}(g\mu_B)^2 \mathcal{S}_{\nu\nu'}(\boldsymbol{q};\omega), \quad n_B(\omega) = \frac{1}{e^{\beta\omega}-1}.$$

Assuming $k_B T$ large and using Eq. (42) we find

$$\mathrm{Re}[\chi_{\nu\nu'}(\boldsymbol{q};\omega=0)] - \mathrm{Re}[\chi_{\nu\nu'}(\boldsymbol{q};\infty)] \sim \frac{(g\mu_B)^2}{k_B T}\mathcal{S}_{\nu\nu'}(\boldsymbol{q};t=0).$$

A.2.4 Imaginary-time and frequency response function

We define the susceptibility in imaginary time as

$$\chi_{\nu\nu'}(\boldsymbol{q};\tau,\tau') = \langle \mathcal{T} \Delta M_\nu(\boldsymbol{q};\tau) \Delta M_{\nu'}(-\boldsymbol{q};\tau')\rangle$$

where $\Delta M_\nu(\boldsymbol{q};\tau) = M_\nu(\boldsymbol{q};\tau) - \langle M_\nu(\boldsymbol{q};0)\rangle$. As in the case of the Green function, by using the invariance properties of the trace one can show that

$$\chi_{\nu\nu'}(\boldsymbol{q};\tau,\tau') = \chi_{\nu\nu'}(\boldsymbol{q};\tau-\tau').$$

The response function in imaginary time is related to the response function at the bosonic Matsubara frequency $i\omega_m$ through the Fourier transforms

$$\chi_{\nu\nu'}(\boldsymbol{q};\tau) = \frac{1}{\beta}\sum_n e^{-i\omega_m\tau}\chi_{\nu\nu'}(\boldsymbol{q};i\omega_m),$$
$$\chi_{\nu\nu'}(\boldsymbol{q};i\omega_m) = \int d\tau e^{i\omega_m\tau}\chi_{\nu\nu'}(\boldsymbol{q};\tau).$$

A.3 Magnetic susceptibility

A.3.1 Spin and magnetization operators

The spin operators S_ν are defined as

$$S_\nu = \frac{1}{2}\sum_{\sigma\sigma'} c^\dagger_\sigma \sigma_\nu c_{\sigma'},$$

where $\nu = x, y, z$ and σ_ν are the Pauli matrices

$$\sigma_x = \begin{pmatrix} 0 & 1 \\ 1 & 0 \end{pmatrix} \quad \sigma_y = \begin{pmatrix} 0 & -i \\ i & 0 \end{pmatrix} \quad \sigma_z = \begin{pmatrix} 1 & 0 \\ 0 & -1 \end{pmatrix}.$$

The magnetization operators M_ν are defined as $M_\nu = -g\mu_B S_\nu$.

A.3.2 Matsubara magnetic susceptibility

The magnetic susceptibility for a single-band system can be expressed as

$$\chi_{zz}(\boldsymbol{q};\boldsymbol{\tau}) = \frac{(g\mu_B)^2}{4}\sum_{\sigma\sigma'}\sigma\sigma'\,\chi^{\boldsymbol{q}\sigma\sigma'}(\boldsymbol{\tau}) = \frac{(g\mu_B)^2}{4}\sum_{\sigma\sigma'}\sigma\sigma'\,\underbrace{\frac{1}{\beta}\frac{1}{N_{\boldsymbol{k}}^2}\sum_{\boldsymbol{k}\boldsymbol{k}'}[\chi(\boldsymbol{q};\boldsymbol{\tau})]_{\sigma\boldsymbol{k},\sigma'\boldsymbol{k}'}}_{\chi^{\boldsymbol{q}\sigma\sigma'}(\boldsymbol{\tau})} \tag{43}$$

where $\sigma = 1$ or -1 depending on whether the spin is up or down, $\boldsymbol{\tau} = (\tau_1, \tau_2\,\tau_3, \tau_4)$ and

$$\begin{aligned}[\chi(\boldsymbol{q};\boldsymbol{\tau})]_{\sigma\boldsymbol{k},\sigma'\boldsymbol{k}'} =& \langle \mathcal{T} c_{\boldsymbol{k}\sigma}(\tau_1) c^\dagger_{\boldsymbol{k}+\boldsymbol{q}\sigma}(\tau_2) c_{\boldsymbol{k}'+\boldsymbol{q}\sigma'}(\tau_3) c^\dagger_{\boldsymbol{k}'\sigma'}(\tau_4)\rangle \\ & - \langle \mathcal{T} c_{\boldsymbol{k}\sigma}(\tau_1) c^\dagger_{\boldsymbol{k}+\boldsymbol{q}\sigma}(\tau_2)\rangle\langle \mathcal{T} c_{\boldsymbol{k}'+\boldsymbol{q}\sigma'}(\tau_3) c^\dagger_{\boldsymbol{k}'\sigma'}(\tau_4)\rangle.\end{aligned}$$

In Fourier space

$$\chi_{zz}(\boldsymbol{q}; i\omega_m) = \frac{(g\mu_B)^2}{4} \sum_{\sigma\sigma'} \sigma\sigma' \frac{1}{\beta^2} \sum_{nn'} \chi^{\boldsymbol{q}\sigma\sigma'}_{n,n'}(i\omega_m)$$
$$= \frac{(g\mu_B)^2}{4} \sum_{\sigma\sigma'} \sigma\sigma' \frac{1}{\beta^2} \sum_{nn'} \underbrace{\frac{1}{\beta}\frac{1}{N_{\boldsymbol{k}}^2} \sum_{\boldsymbol{k}\boldsymbol{k}'} [\chi(\boldsymbol{q}; i\omega_m)]_{\sigma\boldsymbol{k}n,\sigma'\boldsymbol{k}'n'}}_{\chi^{\boldsymbol{q}\sigma\sigma'}_{n,n'}(i\omega_m)},$$

where $\omega_m = 2m\pi/\beta$ is a bosonic Matsubara frequency and

$$\chi^{\boldsymbol{q}\sigma\sigma'}_{n,n'}(i\omega_m) = \chi^{\boldsymbol{q}\sigma\sigma'}(\boldsymbol{\nu}) = \frac{\beta}{8} \iiint d\boldsymbol{\tau}\ e^{i\boldsymbol{\nu}\cdot\boldsymbol{\tau}} \chi^{\boldsymbol{q}\sigma\sigma'}(\boldsymbol{\tau}). \tag{44}$$

The integral for each $\boldsymbol{\tau}$ component is from $-\beta$ to β and $\boldsymbol{\nu} = (\nu_n, -\nu_n - \omega_m, \nu_{n'} + \omega_m, -\nu_{n'})$.

A.3.3 Symmetry properties

Let us now analyze the symmetry properties of (44). The complex conjugate is given by

$$\left[\chi^{\boldsymbol{q}\sigma\sigma'}_{n,n'}(i\omega_m)\right]^* = \chi^{\boldsymbol{q}\sigma\sigma'}_{-n-1,-n'-1}(-i\omega_m),$$

with

$$\chi^{\boldsymbol{q}\sigma\sigma'}_{n,n'}(i\omega_m) = \frac{\beta}{8} \iiint d\boldsymbol{\tau}\ e^{i(-\omega_m\tau_{23}+\nu_n\tau_{12}+\nu_{n'}\tau_{34})} \chi^{\boldsymbol{q}\sigma\sigma'}(\boldsymbol{\tau}).$$

By using the fact that, for the cases considered here, the response function is real in τ space and by exchanging the indices 1 and 4, 2 and 3 in the integrand, we find

$$\chi^{\boldsymbol{q}\sigma\sigma'}_{n,n'}(i\omega_m) = \chi^{\boldsymbol{q}\sigma'\sigma}_{n',n}(i\omega_m),$$

and hence if $\sigma = \sigma'$, $\nu_n = \nu'_n$ is a reflection axis. An additional reflection axis can be found by first shifting the frequency $\nu_n = \nu_l - \omega_m$

$$\chi^{\boldsymbol{q}\sigma\sigma'}_{l,n'}(i\omega_m) = \frac{\beta}{8} \iiint d\boldsymbol{\tau}\ e^{i(-\omega_m\tau_{13}+\nu_l\tau_{12}+\nu_{n'}\tau_{34})} \chi^{\boldsymbol{q}\sigma\sigma'}(\boldsymbol{\tau})$$

and then exchanging in the integrand the indices 12 with 34 and vice versa. Hence

$$\chi^{\boldsymbol{q}\sigma\sigma'}_{l,n'}(i\omega_m) = \chi^{\boldsymbol{q}\sigma'\sigma}_{n',l}(-i\omega_m)$$

so that, if $\sigma = \sigma'$, $\nu_{n+m} = -\nu_{n'}$ is a mirror line

$$\left|\chi^{\boldsymbol{q}\sigma\sigma'}_{n+m,n'}(i\omega_m)\right| = \left|\chi^{\boldsymbol{q}\sigma'\sigma}_{-n'-1,-n-m-1}(i\omega_m)\right|.$$

A.3.4 Non-interacting limit

For a non-interacting system described by Hamiltonian (36) Wick's theorem yields

$$\begin{aligned}\chi^{\boldsymbol{q}\sigma\sigma'}(\boldsymbol{\tau}) &= -\frac{1}{\beta}\frac{1}{N_{\boldsymbol{k}}}\sum_{\boldsymbol{k}}\langle\mathcal{T}c_{\boldsymbol{k}\sigma}(\tau_1)c^{\dagger}_{\boldsymbol{k}+\boldsymbol{q}\sigma'}(\tau_4)\rangle\langle\mathcal{T}c_{\boldsymbol{k}+\boldsymbol{q}\sigma'}(\tau_3)c^{\dagger}_{\boldsymbol{k}\sigma}(\tau_2)\rangle \\ &= -\frac{1}{\beta}\frac{1}{N_{\boldsymbol{k}}}\sum_{\boldsymbol{k}}\mathcal{G}_{\boldsymbol{k}\sigma}(\tau_{14})\mathcal{G}_{\boldsymbol{k}+\boldsymbol{q}\sigma'}(-\tau_{23})\delta_{\sigma,\sigma'}.\end{aligned}$$

Then, in the paramagnetic case, the magnetic susceptibility is given by

$$\chi_{zz}(\boldsymbol{q};\boldsymbol{\tau}) = -(g\mu_B)^2\frac{1}{4}\frac{1}{\beta}\frac{1}{N_{\boldsymbol{k}}}\sum_{\boldsymbol{k}\sigma}\mathcal{G}_{\boldsymbol{k}\sigma}(\tau_{14})\mathcal{G}_{\boldsymbol{k}+\boldsymbol{q}\sigma}(-\tau_{23}).$$

Its Fourier transform is

$$\chi_{zz}(\boldsymbol{q};i\omega_m) = (g\mu_B)^2\frac{1}{4}\frac{1}{\beta^2}\sum_{nn'}\sum_{\sigma}\chi^{\boldsymbol{q}\sigma\sigma}_{n,n'}(i\omega_m),$$

where

$$\sum_{\sigma}\chi^{\boldsymbol{q}\sigma\sigma}_{n,n'}(i\omega_m) = -\beta\frac{1}{N_{\boldsymbol{k}}}\sum_{\boldsymbol{k}\sigma}\mathcal{G}_{\boldsymbol{k}\sigma}(i\nu_n)\mathcal{G}_{\boldsymbol{k}+\boldsymbol{q}\sigma}(i\nu_n+i\omega_m)\delta_{n,n'}.$$

Thus, the static susceptibility is

$$\chi_{zz}(\boldsymbol{q};0) = -\left(g\mu_B\right)^2\frac{1}{4}\frac{1}{N_{\boldsymbol{k}}}\sum_{\boldsymbol{k}\sigma}\frac{n_\sigma(\varepsilon_{\boldsymbol{k}+\boldsymbol{q}})-n_\sigma(\varepsilon_{\boldsymbol{k}})}{\varepsilon_{\boldsymbol{k}+\boldsymbol{q}}-\varepsilon_{\boldsymbol{k}}}.$$

Finally, in the $\boldsymbol{q}\to 0$ and $T\to 0$ limit we find

$$\chi_{zz}(\mathbf{0};0) = \frac{1}{4}\left(g\mu_B\right)^2\underbrace{\frac{1}{N_{\boldsymbol{k}}}\sum_{\boldsymbol{k}\sigma}\left[-\frac{dn_\sigma(\varepsilon_{\boldsymbol{k}})}{d\varepsilon_{\boldsymbol{k}}}\right]_{T=0}}_{\rho(\varepsilon_F)} = \frac{1}{4}\left(g\mu_B\right)^2\rho(\varepsilon_F).$$

A.3.5 Atomic limit

In the atomic limit, we sum over $\boldsymbol{q}$ to obtain the local susceptibility tensor

$$\chi^{\sigma\sigma'}(\boldsymbol{\tau}) = \frac{1}{N_{\boldsymbol{k}}}\sum_{\boldsymbol{q}}\chi^{\boldsymbol{q}\sigma\sigma'}(\boldsymbol{\tau}).$$

For Hamiltonian (38), in the sector $\boldsymbol{\tau}^+$ such that $\tau_i > \tau_{i+1}$, the latter has the form

$$\chi^{\sigma\sigma'}(\boldsymbol{\tau}^+) = \frac{1}{\beta}\frac{1}{2(1+e^{\beta U/2})}\left(e^{\tau_{12}U/2+\tau_{34}U/2}+\delta_{\sigma\sigma'}e^{(\beta-\tau_{12})U/2-\tau_{34}U/2}\right).$$

The magnetic susceptibility for $\tau_i > \tau_{i+1}$ is then given by

$$\chi_{zz}(\boldsymbol{\tau}^+) = (g\mu_B)^2\frac{1}{4}\sum_{\sigma\sigma'}\sigma\sigma'\chi^{\sigma\sigma'}(\boldsymbol{\tau}^+) = \frac{(g\mu_B)^2}{4\beta}\frac{1}{(1+e^{\beta U/2})}e^{(\beta-\tau_{12}-\tau_{34})U/2},$$

which depends only on $\tau = \tau_{12}+\tau_{34}$. In the remaining sectors (labeled with P) the susceptibility has a similar form after appropriate permutation of the imaginary times

$$\chi_{zz}(\boldsymbol{\tau}^P) = (g\mu_B)^2 \frac{1}{4} \sum_{\sigma\sigma'} \sigma\sigma' \chi^{\sigma\sigma'}(\boldsymbol{\tau}^P) = s_P \frac{(g\mu_B)^2}{4\beta} n(-s_P\, y) e^{-s_P(\tau_{12}+\tau_{34})y},$$

where $y = U/2$ and $s_P = \pm 1$; the derivation can be found in [27]. If we perform the Fourier transform of $\chi_{zz}(\boldsymbol{\tau})$ we find $\chi_{zz}(i\omega_n) = \chi_{zz}(0)\delta_{\omega_n,0}$. The static susceptibility is

$$\chi_{zz}(0) = (g\mu_B)^2 \frac{1}{4k_BT} \frac{e^{\beta U/2}}{1+e^{\beta U/2}} = (g\mu_B)^2 \frac{1}{4} \frac{1}{\beta^2} \sum_{nn'} \sum_{\sigma\sigma'} \sigma\sigma'\, \chi^{\sigma\sigma'}_{n,n'}(0).$$

Here, after setting

$$M_n = \left[\frac{1}{i\nu_n - y} - \frac{1}{i\nu_n + y} \right]$$

we have

$$\begin{aligned} \sum_{\sigma\sigma'} \sigma\sigma'\, \chi^{\sigma\sigma'}_{n,n'}(0) =& \frac{dM_{n'}M_n}{dy} - \beta n(y) \left[\delta_{n,n'} \frac{dM_n}{dy} + \delta_{n,-n'-1} \frac{dM_{n'}}{dy} \right] + \beta n(-y) M_n M_{n'} \\ & - \frac{1}{y} \left[M_{n'} - \beta n(y) \delta_{n,-n'-1} + \beta n(-y) \delta_{n,n'} \right] M_n. \end{aligned}$$

Most contributions cancel each other when the sums over the Matsubara frequencies are performed. A detailed derivation can be found in Ref. [27]. For $y = 0$ only the terms proportional to $\delta_{n,n'}$ survive, as expected from the Wick theorem.

References

[1] P. Weiss, J. Phys. Theor. Appl. **6**, 661 (1907)

[2] F. Hund, Z. Phys. **33**, 855 (1925)

[3] W. Heisenberg, Z. Phys. **49**, 619 (1928)

[4] C.G. Shull and J.S. Smart, Phys. Rev. **76**, 1256 (1949)

[5] L. Néel, Ann. de Phys. **17**, 5 (1932); *ibid.* **5**, 232 (1936); C. R. Acad. Sc. **203**, 304 (1936)

[6] H. Bethe, Z. Phys. **71**, 205 (1931)

[7] P.W. Anderson, Phys. Rev. **86**, 694 (1952)

[8] P.W. Anderson, Phys. Rev. **130**, 439 (1963)

[9] P.W. Higgs, Phys. Rev. Lett. **13**, 508 (1964)

[10] J. Kondo, Prog. Theor. Phys. **32**, 37 (1964)

[11] K. Andres, J.E. Graebner and H.R. Ott, Phys. Rev. Lett. **35**, 1779 (1975)

[12] A.C. Hewson: *The Kondo Problem to Heavy Fermions*
(Cambridge University Press, 1993)

[13] J.G. Bednorz, K.A. Müller, Z. Phys. B **64**, 189 (1986)

[14] W. Metzner and D. Vollhardt, Phys. Rev. Lett. **62**, 324 (1989);
A. Georges and G. Kotliar, Phys. Rev. B **45**, 6479 (1992)

[15] E. Pavarini, E. Koch, A. Lichtenstein, D. Vollhardt:
The LDA+DMFT approach to strongly correlated materials,
Reihe Modeling and Simulation, Vol. 1 (Forschungszentrum Jülich, 2011)
`http://www.cond-mat.de/events/correl11`

[16] E. Pavarini, E. Koch, A. Lichtenstein, D. Vollhardt: *DMFT at 25: Infinite Dimensions*,
Reihe Modeling and Simulation, Vol. 4 (Forschungszentrum Jülich, 2014)
`http://www.cond-mat.de/events/correl14`

[17] H. Bruus and K. Flensberg: *Many-Body Quantum Theory in Condensed Matter Physics*
(Oxford University Press, 2004)

[18] P. Fazekas: *Lecture Notes on Electron Correlation and Magnetism*
(World Scientific, Singapore, 1999)

[19] D.C. Matthis: *The Theory of Magnetism Made Simple* (World Scientific, Singapore, 2006)

[20] K. Yosida: *Theory of Magnetism* (Springer, Heidelberg, 1998)

[21] E. Pavarini, E. Koch, F. Anders, M. Jarrell:
Correlated electrons: from models to materials,
Reihe Modeling and Simulation, Vol. 2 (Forschungszentrum Jülich, 2012)
`http://www.cond-mat.de/events/correl12`

[22] E. Pavarini, E. Koch, U. Schollwöck:
Emergent Phenomena in Correlated Matter,
Reihe Modeling and Simulation, Vol. 3 (Forschungszentrum Jülich, 2013)
`http://www.cond-mat.de/events/correl13`

[23] See R. Eder, *Multiplets in Transition Metal Ions* in Ref. [21]

[24] See E. Pavarini, *Crystal-field Theory, Tight-binding Method and Jahn-Teller Effect*, in Ref. [21]

[25] See E. Pavarini, *The LDA+DMFT Approach*, in Ref. [15]

[26] See E. Koch, *Exchange Mechanisms*, in Ref. [21]

[27] See E. Pavarini, *Linear-response Theory*, in Ref. [16]

[28] J.R. Schrieffer and P.A. Wolff, Phys. Rev. **149**, 491 (1966);
A.H. MacDonald, S.M. Girvin and D. Yoshioka, Phys. Rev. B **37**, 9753 (1988)

[29] E. Pavarini, I. Dasgupta, T.Saha-Dasgupta, O. Jepsen and O.K. Andersen,
Phys. Rev. Lett. **87**, 047003 (2001)

[30] K. Wilson, Rev. Mod. Phys. **47**, 773 (1975)

[31] N. Andrei, K. Furuya, and J.H. Lowenstein, Rev. Mod. Phys. **55**, 331 (1983);
A.M. Tsvelik and P.B. Wiegmann, Adv. Phys. **32**, 453 (1983)

[32] J.E. Gubernatis, J.E. Hirsch, and D.J. Scalapino, Phys. Rev. B **16**, 8478 (1987)

[33] P.W. Anderson, J. Phys. C: Solid State Phys. **3**, 2436 (1970)

[34] E. Pavarini and L.C. Andreani, Phys. Rev. Lett. **77**, 2762 (1996)

[35] P. Nozières, J. Low. Temp. Phys. **17**, 31 (1974)

[36] A.I. Lichtenstein, M.I. Katsnelson, and V.A. Gubanov, J. Phys. F **14**, L125;
Solid State Commun. **54**, 327 (1985);
A.I. Lichtenstein, M.I. Katsnelson, V.P. Antropov, and V.A. Gubanov,
J. Magn. Magn. Mater. **67**, 65 (1987);
M.I. Katsnelson and A.I. Lichtenstein, Phys. Rev. B **61**, 8906 (2000)

[37] E. Pavarini, E. Koch, and A.I. Lichtenstein,
Phys. Rev. Lett. **101**, 266405 (2008);
A. Chiesa, S. Carretta, P. Santini, G. Amoretti and E. Pavarini,
Phys. Rev. Lett. **110**, 157204 (2013)